OCS Study
BOEM 2022-015

California North Coast Offshore Wind Study: Wind Speed Resource and Power Generation Profile Augmentation Report

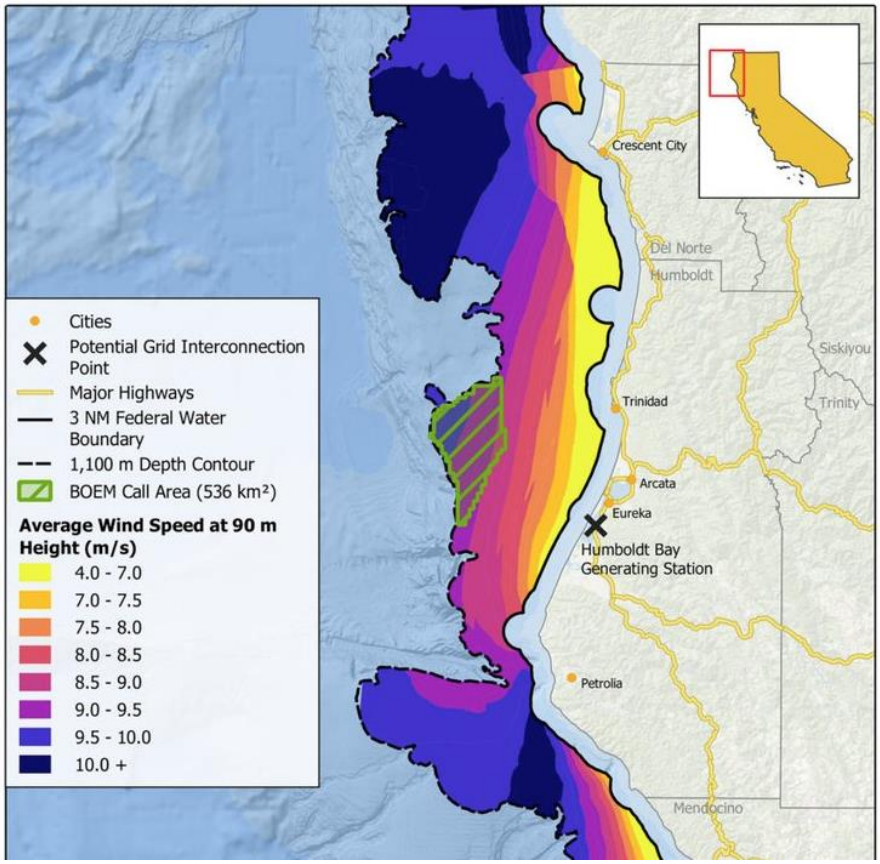

This report was prepared by Amin Younes, Charles Chamberlin, and Arne Jacobson of the Schatz Energy Research Center. It was published by the Schatz Energy Research Center in March 2022.

Schatz Energy Research Center
Cal Poly Humboldt
Arcata, CA 95521 | (707) 826-4345

Schatz Energy Research Center

BOEM Bureau of Ocean Energy Management

Disclaimer

Study collaboration and funding were provided by the U.S. Department of the Interior, Bureau of Ocean Energy Management (BOEM), Pacific Regional Office, Camarillo, CA, under Agreement Number M19AC00005. This report has been technically reviewed by BOEM, and it has been approved for publication. The views and conclusions contained in this document are those of the authors and should not be interpreted as representing the opinions or policies of the U.S. Government, nor does mention of trade names or commercial products constitute endorsement or recommendation for use.

Report Availability

To download a PDF file of this report, go to the U.S. Department of the Interior, Bureau of Ocean Energy Management, Recently Completed Environmental & Technical Studies – Pacific webpage (https://www.boem.gov/recently-completed-environmental-studies-pacific), and click on the link for OCS Report #2022-015.

The report is also available on the Schatz Energy Research Center website at: schatzcenter.org/publications

About the Schatz Energy Research Center

The Schatz Energy Research Center at Cal Poly Humboldt advances clean and renewable energy. Our projects aim to reduce climate change and pollution while increasing energy access and resilience.

Our work is collaborative and multidisciplinary, and we are grateful to the many partners who together make our efforts possible.

Learn more about our work at schatzcenter.org

Rights and Permissions

The material in this work is subject to copyright. Please cite as follows:

Younes, A., C. Chamberlin, A. Jacobson. (2022). *California North Coast Offshore Wind Study: Wind Speed Resource and Power Generation Profile Augmentation Report*. Cal Poly Humboldt, Arcata, CA: Schatz Energy Research Center. schatzcenter.org/publications/

All images remain the sole property of their source and may not be used for any purpose without written permission from that source.

EXECUTIVE SUMMARY

This report documents updates to our previous California north coast offshore wind resource assessment, which assessed the power generation potential of offshore wind within the Bureau of Ocean Energy Management (BOEM) Humboldt Call Area[1] at scales of 48 MW, 144 MW, and 1,836 MW and at a notional Cape Mendocino area at scales of 144 MW and 1,836 MW (Severy et al., 2020). This study expands on that work in four important ways:

First, this resource assessment relies on a new model of offshore wind speeds, herein referred to as the CA20 dataset (Optis et al., 2020), replacing the previously used Wind Integration National Dataset (WIND) Toolkit (NREL, n.d.). The CA20 dataset provides twenty years of data, from 2000 through 2019, compared to the WIND Toolkit's eight-year period of record, 2007 to 2014. The two models also use different planetary boundary layer schemes, resulting in different wind speed distributions and profiles.

Second, we have updated the turbine mathematical model based on the latest assessment by NREL (Beiter et al., 2020). The primary differences are a cut-out speed increase from 25 up to 30 meters per second and a hub height increase from 136 m up to 138 m, both which increase generation.

Third, this analysis provides an assessment of wind farms between 144 MW and 1,836 MW, at intermediate sizes of 288 MW and 480 MW.

Fourth and finally, we assess more regions. In the previous study all developments assessed power generation at the centroids of the Humboldt Call Area or a hypothetical area offshore from Cape Mendocino, while this study explores an additional notional area that is offshore from Crescent City. We also explore two additional notional locations within and one just outside and to the east of the Humboldt Call Area (the "Humboldt Study Area") to enable evaluation of the tradeoff between higher development costs associated with deeper waters and increased distance to shore versus increased generation due to higher wind speeds further from shore.

This report is grouped into three Studies: A, B, and C. In Study A, we compare our original analysis (Severy et al., 2020) using the WIND Toolkit wind speed data to a new analysis using the CA20 wind speed dataset and the new turbine power curve and hub height. This includes assessment of wind farm performance at the Humboldt Call Area and the notional Cape Mendocino area at the previously studied scales of 48 MW (Humboldt only), 144 MW, and 1,836 MW. In Study B, we provide analysis of wind farm performance at three locations within the Humboldt Call Area at scales of 48 MW to 480 MW. In Study C, we compare performance of wind farms located in all three areas (the Humboldt Call Area, notional Cape Mendocino area, and notional Crescent City area) at all five studied sizes, as well as a 48-MW development in a hypothetical Humboldt Study Area located just east of the Humboldt Call Area.

Study A: Humboldt Call Area and notional Cape Mendocino area update

The updated CA20 dataset results in more frequent predictions of higher wind speeds at both the Humboldt Call Area and the notional Cape Mendocino area. Significantly, the divergence in empirical cumulative distribution functions begins at about 11 meters per second in the Notional Cape Mendocino area, and closer to 9 meters per second in the Humboldt Call Area (see Figure

[1] The Humboldt Call Area has been identified by the Bureau of Ocean Energy Management (2018b), and this term is used throughout this report. BOEM has since changed the name to the Humboldt Wind Energy Area.

ES-1). Because the turbines are at rated speed at 11 meters per second, and thus no longer produce more power with increased speed, the new model (including updated turbine power curve and hub heights) has little effect on predicted power generation at the notional Cape Mendocino area, while predicting 5 to 6% greater power output in the Humboldt Call Area than the previous model. This reduces the power production advantage in the notional Cape Mendocino area from 17% to 10 to 11% (depending upon development size).

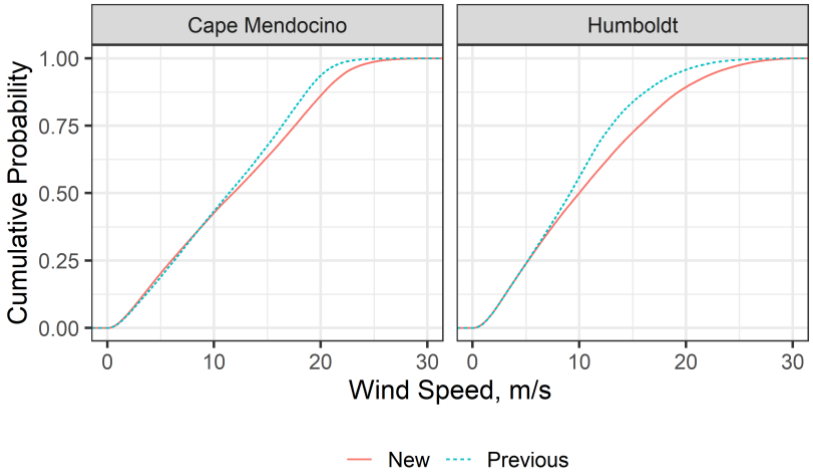

Figure ES-1. Comparison of previous and new cumulative probability distribution functions of wind speed in both locations. Wind speeds are at the turbine hub heights, 136 m for the previous analysis and 138 m for the new analysis.

Study B: Variation across the Humboldt Call Area

Study B explored the changes in wind speed and power production moving across the Humboldt Call Area from the centroid of a hypothetical east-adjacent farm to that of a hypothetical west-adjacent 480 MW farm (1/3 of the call area apart). Differences in wind speeds are barely visible in Figure ES-2, while power production differs by only 2%. Across the entire width of the Humboldt Call Area, power production would vary up to 5%.

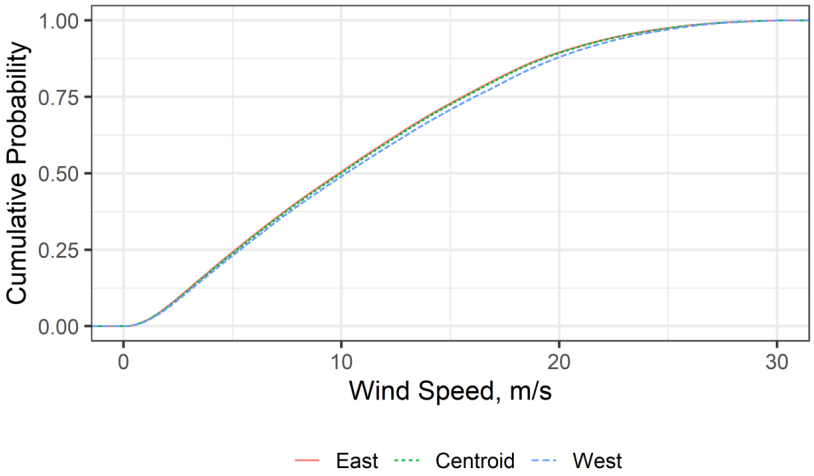

Figure ES-2. Cumulative distribution function of wind speed in the three Humboldt Call Area locations at a turbine hub height of 138 m.

Study C: Comparison between a notional Cape Mendocino area, a notional Crescent City area, the Humboldt Call Area, and a notional Humboldt Study Area

On average, the notional Cape Mendocino area, the most powerful location, provides 16% more energy than the notional Humboldt Study Area, 10 to 11% more than the Humboldt Call Area, and 5% more than the notional Crescent City area (Table ES-1).

Table ES-1. Annual energy production for 48-MW wind farms at Study C locations using the CA20 dataset and new turbine power curve and wake losses. n = 20 years.

Region	95% Confidence Interval for Population Mean (GWh per year)	95% Tolerance Interval (GWh per year)
Cape Mendocino	242 +/- 5.39	210 - 273
Crescent City	230 +/- 4.59	203 - 257
Humboldt Call Area	219 +/- 5.47	187 - 251
Humboldt Study Area	208 +/- 5.57	175 - 241

Figure ES-3 shows the number of hours each year that a 48-MW wind farm would produce at or above a given power level. While all four sites generate no power for the same amount of time, there is a steady decrease in time spent at full power moving from the notional Cape Mendocino area to the notional Crescent City area, to the Humboldt Call Area, and finally the Humboldt Study Area.

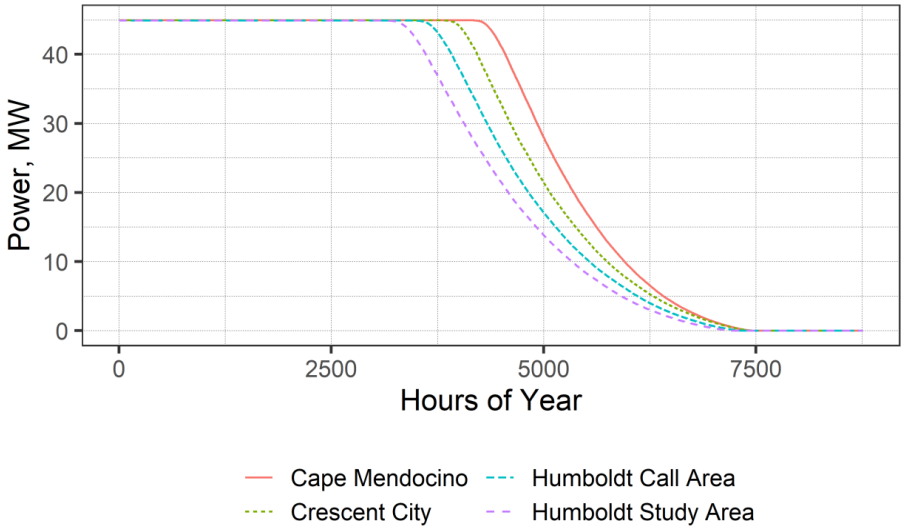

Figure ES-3. Generation duration curves for all four Study C locations at a scale of 48 MW.

Conclusions and Next Steps

In our newest analysis, the power output gap between the notional Cape Mendocino area and the Humboldt Call Area has shrunk significantly, from 17% to 10 to 11%, due to the increased wind

speeds predicted by the CA20 model providing more benefit at the Humboldt Call Area based on the turbine power curves we utilized. In addition to raising the relative value of developments at the Humboldt Call Area, this highlights the potential value of developing and deploying wind turbines with a power curve that is tailored to these wind regimes (i.e., so that there is greater ability to take advantage of the higher wind speeds). This could prove a valuable topic for future research, potentially leading to decreased costs for wind energy offshore of California.

There is potential benefit to a study of more possible locations and more development sizes within the Humboldt Call Area and the other hypothetical call areas. Such studies could be used to inform cost-benefit analyses exploring the tradeoffs of higher wind speed and higher development (and operations and maintenance) costs further from shore.

Finally, it will be beneficial to validate the CA20 model using lidar data from the recently deployed offshore buoys near the Humboldt Call Area and Morro Bay, which began collecting data in September and October of 2020 (Showalter, 2020). Such a comparison will be possible about one year after deployment, though recent damage to the buoy offshore of Humboldt could delay such an endeavor (Gorton, 2021).

TABLE OF CONTENTS

1 INTRODUCTION AND PURPOSE

The purpose of this report is to document the methods and results associated with updating our previous California north coast offshore wind resource assessment (Severy et al., 2020). Severy et al. assessed power generation potential of offshore wind within the Humboldt Call Area[2] (Bureau of Ocean Energy Management, 2018a, 2018b) at scales of 48 MW, 144 MW, and 1,836 MW and at a notional Cape Mendocino area at scales of 144 MW and 1,836 MW. This study expands on Severy et al. (2020) in four important ways:

First, the resource assessment relies on a new model of offshore wind speeds, herein referred to as the CA20 dataset (Optis et al., 2020), replacing the previously used Wind Integration National Dataset (WIND) Toolkit (NREL, n.d.). The CA20 dataset provides twenty years of data, from 2000 through 2019, compared to the WIND Toolkit's eight-year period of record, 2007 to 2014. The two models also use different planetary boundary layer (PBL) schemes. "The WIND Toolkit used the Yonsei University (YSU) scheme, whereas the CA20 data set uses the Mellor-Yamada-Nakanishi-Niino (MYNN) scheme" (Optis et al., 2020, p. vi). Importantly, there is a "tendency for the MYNN scheme to model much higher wind shear below 50 m relative to the YSU scheme" (Optis et al., 2020, p. 11), leading to differences in the wind shear profile and the resulting wind speed distributions. This resource model is believed to provide more representative data, but since there are limited directly comparable measurements, this has not yet been proven. A lidar buoy was deployed 20 miles offshore of Humboldt County (location 40.9708° N 124.5901° W) (Showalter, 2020) which measures wind speeds at heights up to 160 m. These data became available starting in early October 2020 (Gorton, 2020a). Another buoy is present a similar distance off the coast of Morro Bay (location 35.71108° N 121.86584° W) (Showalter, 2020), providing a similar set of data (Gorton, 2020b). These buoys will provide sufficient data after about a year of service to allow direct comparison with the two wind shear models, though recent damage to the buoy offshore of Humboldt could delay such an endeavor (Gorton, 2021).

Second, we have updated the turbine power curves based on the latest assessment by NREL (Beiter et al., 2020), as depicted in Figure 1. The primary difference between the new and previous power curves is an extension of the rated power region to 30 meters per second, whereas it was previously assumed that the wind turbines would have to curtail generation at wind speeds exceeding 25 meters per second. As Beiter et al. write:

> Typically, a 25-m/s cut-out wind speed is sufficient to capture the vast majority of the available winds . . . but the new offshore wind resource assessment of California has revealed that many of the California sites on the OCS have a significant fraction of average wind speeds above 25 m/s. The resulting lost energy warrants that the reference power curves be modified by extending cut-out wind speed to 30 m/s. . . . We consider this increase of the cut-out wind speed from 25 m/s to 30 m/s a low-risk modification and a relatively minor design change that can be accommodated by the turbine designers if the conditions are known in advance. (Beiter et al., 2020)

[2] The Humboldt Call Area identified by the Bureau of Ocean Energy Management (2018b) is located west of Humboldt Bay, approximately 20 to 30 nautical miles (37-56 km) offshore. The term Humboldt Call Area is used throughout this report. BOEM has since changed the name to the Humboldt Wind Energy Area.

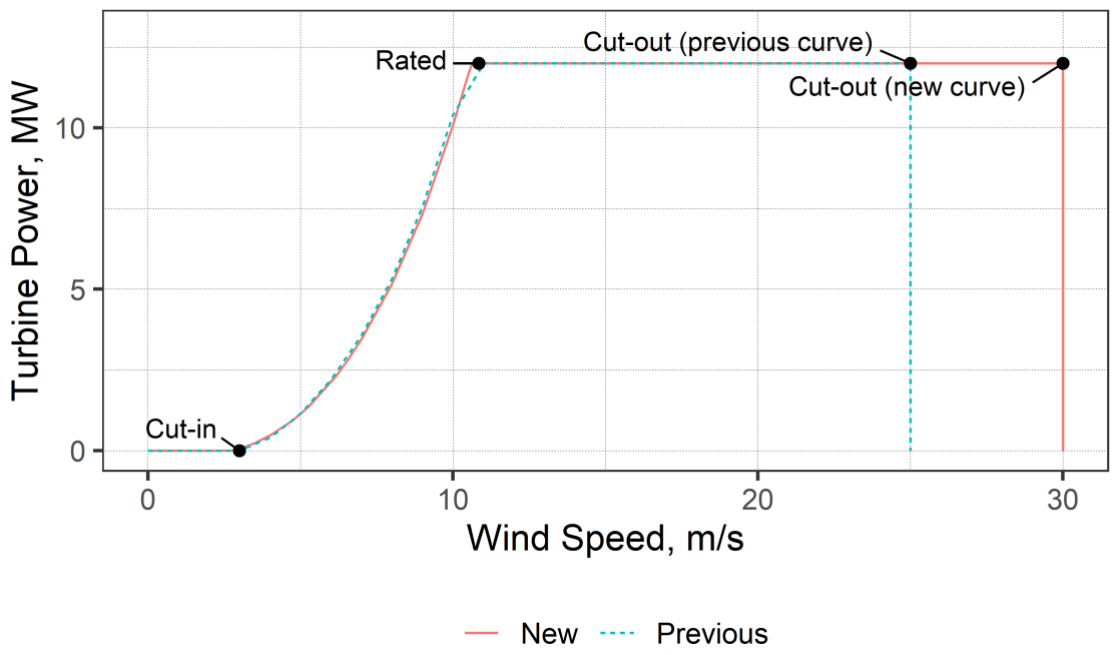

Figure 1. Comparison of two power curves for a 12-MW turbine, adapted from Musial et al. (2019) and Beiter et al. (2020).

The new reference turbine also has a hub height of 138 m, 2 m higher than the previously assumed height. These changes to the turbine power curve and hub height result in a 4.0% increase in power generation (before losses are considered) across the period of record at the Humboldt Call Area centroid, using the new CA20 dataset and analysis methodology.

The third important augmentation in this analysis is additional assessment of wind farms between 144 MW and 1,836 MW. This study includes assessment of all three previous development sizes, 48 MW, 144 MW and 1,836 MW, as well as intermediate sizes of 288 MW (24 x 12-MW turbines), and 480 MW (40 x 12-MW turbines).

Fourth and finally, a third region is now being assessed, as shown in Figure 2. While in the previous study all developments assessed power generation at the centroids of the Humboldt Call Area and a notional area offshore from Cape Mendocino, this study explores an additional notional area that is offshore from Crescent City.

Relating to the Humboldt Call Area specifically, we also explore two additional locations within and one just outside to the east. These points are the centroids of: 1) a 480-MW wind farm adjacent to the west side of the call area, where wind speeds are the highest; 2) a 480-MW farm adjacent to the east side, closest to point of connection; and 3) a 48-MW study-sized farm just outside the eastern boundary of the call area. The goal of studying the performance of wind farms centered at these points is to understand the tradeoff between higher development costs associated with deeper waters and increased distance to shore versus increased generation due to higher wind speeds further from shore. These added study areas are depicted in Figure 3.

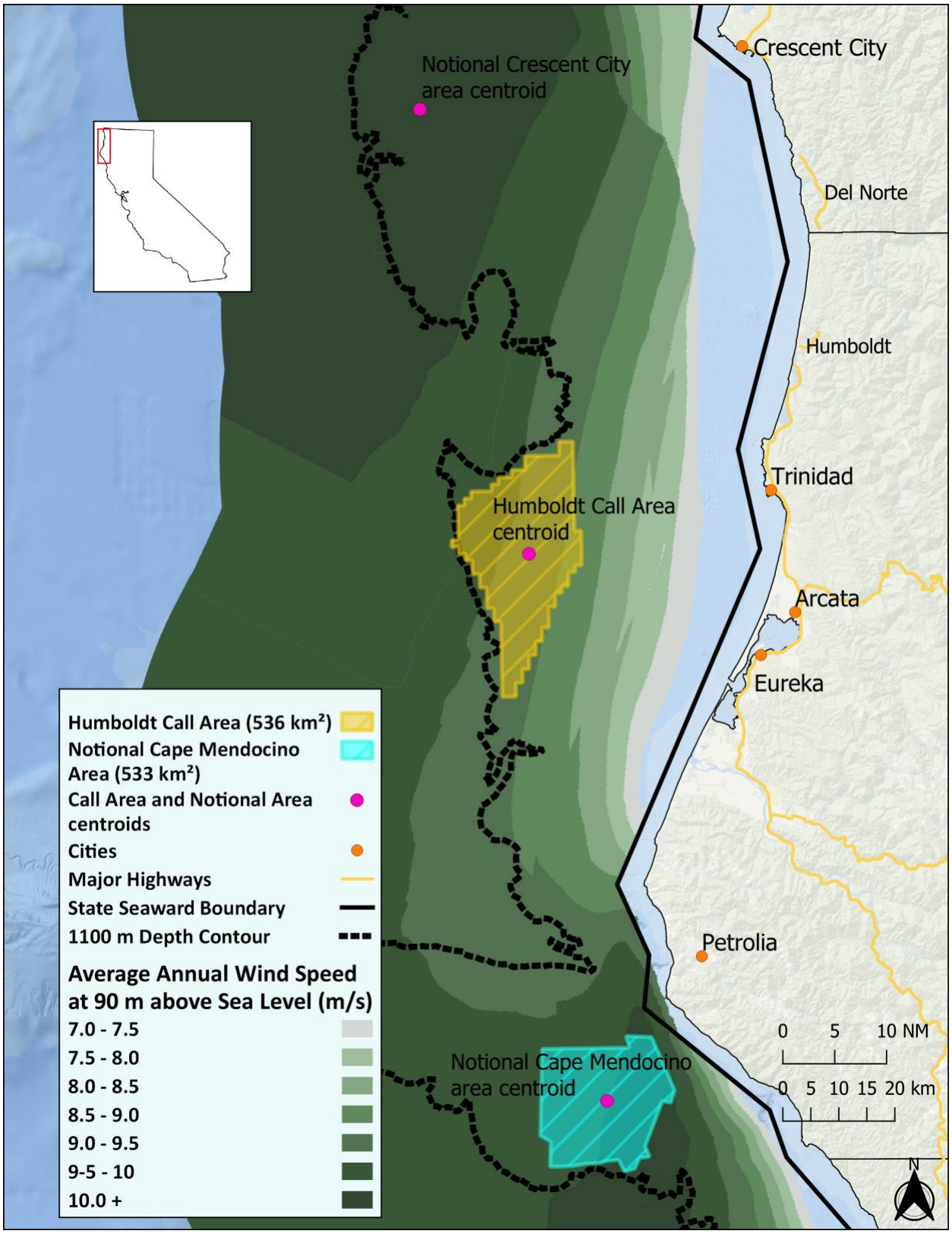

Figure 2. Offshore wind speeds and prospective study regions. Pink dots indicate the centroids of the study regions. Orange dots indicate nearby cities and towns.

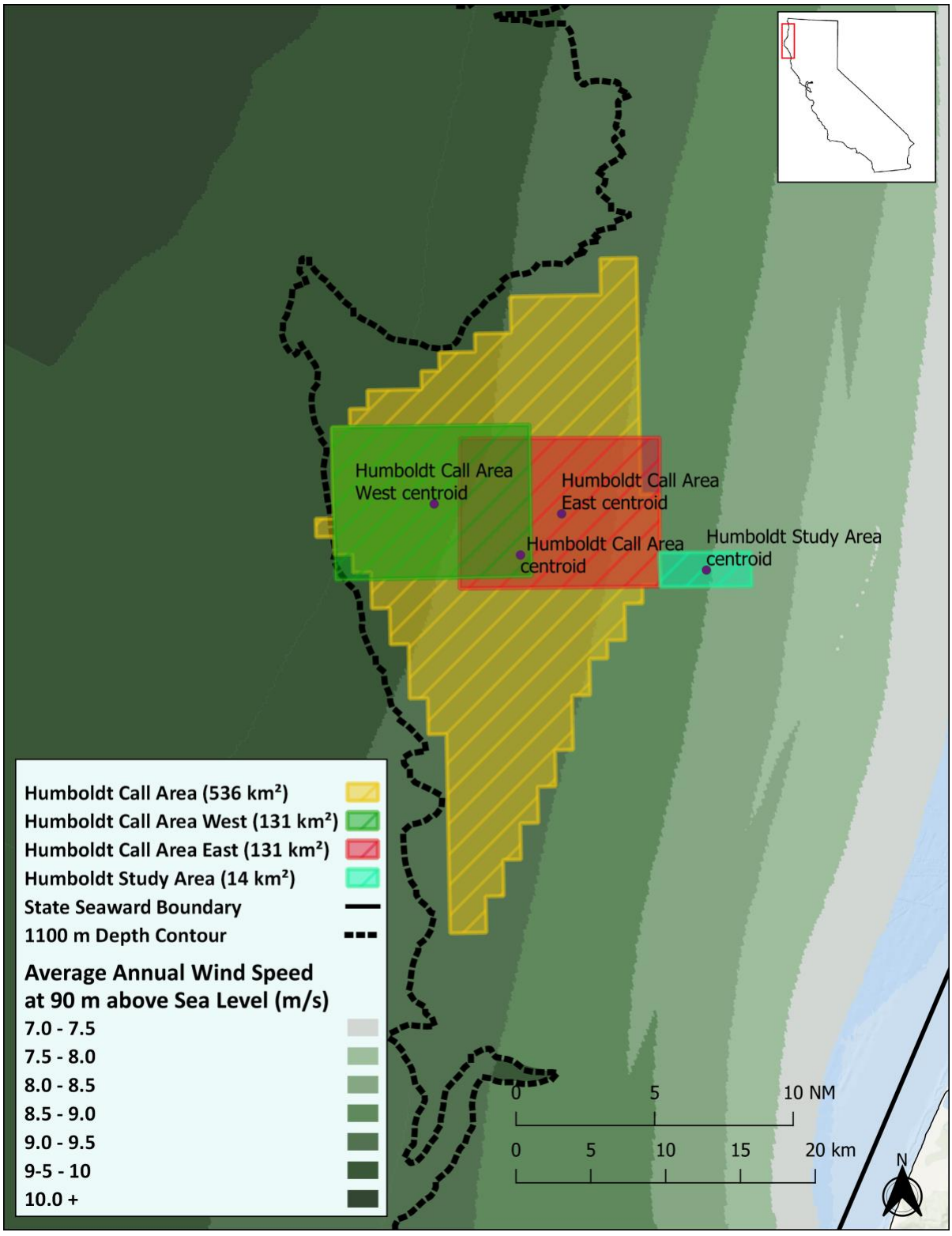

Figure 3. Centroids of the additional Humboldt Call Area hypothetical wind farms, as well as the centroid of a hypothetical study area to the east of the Call Area are depicted as purple dots.

Because the areas are relatively large, the distance between the eastern and western centroids is only about 1/3 of the distance across the call area. It is later shown that the difference in generation between these two points is 2% (Section 4.2.2), while the difference across the whole call area is 5% (Appendix A). Because these changes are relatively small, and linear, we believe that these two points serve as appropriate references.

The chosen shape and layout of the wind farms positioned at these centroids is also significant. Increasing the number of turbines in the N-S direction while decreasing it in the E-W direction would allow the development centroids to shift east or west, lowering project cost or increasing generation, respectively. Because – as shown in Section 4.2.2 – capacity factor varies little between locations and layouts, the net benefit of such a change would be small and would require a focused study to evaluate.

2 SCENARIOS

This report addresses three separate sets of study scenarios (presented in this section as Studies A, B, and C) and of study results (Section 4). First, in Study A, we compare the results of our original analysis (Severy et al., 2020) using the original WIND Toolkit wind speed data to a new analysis using the CA20 wind speed dataset and the new turbine power curve. This includes assessment of wind farm performance at the centroid of the hypothetical Cape Mendocino area at scales of 144 MW and 1,836 MW, and comparison to results at the centroid of the Humboldt Call Area at scales of 48 MW, 144 MW, and 1,836 MW. The reanalysis includes some small changes to the methods, which are noted as they come up in Section 3, but it is otherwise very similar to the original version. Second, in Study B, we provide results required for Task 2.1: Analysis of the wind farm performance at the three locations within the Humboldt Call Area at scales of 48 MW, 144 MW, 288 MW, and 480 MW. Third and finally, in Study C, we compare performance of wind farms located at the centroids of all three areas (the Humboldt Call Area, a notional Mendocino area, and a notional Crescent City area) at all five studied sizes, as well as a comparison to a hypothetical research area located just outside of the eastern edge of the Humboldt Call Area, which we call the notional Humboldt Study Area.

This section provides a summary of the scenario names, nameplate capacities, locations, turbines, and turbine layouts for the scenarios considered. Scenario names and wind farm nameplate capacities are broken down by study.

2.1 Study A Scenarios

Study A includes the exact scenarios from our previous study (Severy et al., 2020): Three scales of development in Humboldt, and two in a notional Cape Mendocino area, as shown in Table 1.

Table 1. Scenarios for Study A.

Nameplate	Humboldt Call Area Centroid	Notional Cape Mendocino Area Centroid
48 MW	H-48	-
144 MW	H-144	M-144
1,836 MW	H-1836	M-1836

2.2 Study B Scenarios

As depicted in Table 2, Study B includes three locations within the Humboldt Call Area at scales from 48 MW to 480 MW. The three positions are shown in Figure 3, above.

Table 2. Scenario codes for Study B by nameplate capacity and location

Nameplate	Humboldt Call Area West	Humboldt Call Area Centroid	Humboldt Call Area East
48 MW	W-48	H-48	E-48
144 MW	W-144	H-144	E-144
288 MW	W-288	H-288	E-288
480 MW	W-480	H-480	E-480

2.3 Study C Scenarios

Study C includes all development sizes at all three centroidal locations, plus a point outside the Humboldt Call Area studied only at pilot (48 MW) scale. Scenarios are tabulated in Table 3

Table 3. Scenarios for study C by nameplate capacity and location

Nameplate	Humboldt Call Area	Humboldt Study Area	Cape Mendocino	Crescent City
48 MW	H-48	HSA-48	M-48	C-48
144 MW	H-144	-	M-144	C-144
288 MW	H-288	-	M-288	C-288
480 MW	H-480	-	M-480	C-480
1,836 MW	H-1836	-	M-1836	C-1836

2.4 Wind Farm Specifications

Wind farms specifications and other design assumptions that are relevant to this analysis are described below.

2.4.1 Locations

Locations include three inside the Humboldt Call Area (West, Centroid, East), one outside the Humboldt Call Area on the eastern side, and one each at the centroids of the notional Cape Mendocino and Crescent City areas. Locations are shown in Figure 2. Coordinates are tabulated in Table 4.

Table 4. Scenario locations and coordinates. The coordinates given are from the CA20 dataset. The points are not identical to those in the Wind Toolkit, with differences between 0.05 and 1.7 km across the studied points.

Region	Position	Latitude	Longitude
Humboldt Call Area	West	40.991°	-124.718°
Humboldt Call Area	Centroid	40.961°	-124.650°
Humboldt Call Area	East	40.986°	-124.615°
Humboldt Call Area	Study Area	40.952°	-124.503°
Cape Mendocino	Centroid	40.094°	-124.487°
Crescent City	Centroid	41.657°	-124.878°

2.4.2 Turbine

All wind farms are assumed to use a 12 MW (nameplate capacity) turbine. This turbine size was selected based on interviews with developers who indicated they would likely deploy turbines rated at 12 MW or larger in the Northern California Call Area. The specifications for this turbine are derived from the most recent version of the standard reference turbine curve developed by NREL (Beiter et al., 2020). The turbine specifications are outlined in Table 5, and its power curve is shown in Figure 1 as the "New" curve. The only significant difference from the former curve is that the turbine cut-out speed has been increased from 25 meters per second to 30 meters per second, while the interpolated points during ramp-up in power also vary slightly.

Table 5. Turbine specifications.

Rated Power	Hub Height	Rotor Diameter
12 MW	138 m[a]	222 m[b]

[a] Source: Beiter et al. (2020). The previous study used a turbine height of 136 m.

[b] Source: Musial et al. (2019). Beiter et al. (2020) use a rotor diameter of 215 m, which would have slightly altered our turbine layouts had we used it.

2.4.3 Wind Farm Turbine Layout

All wind farms of the same capacity have the same number of turbines and the same array shape, as given in Table 6, except for the 1,836 MW developments which are adjusted so that they fit within the areas shown in Figure 2. These shapes are based on the bathymetry for Cape Mendocino and Humboldt, following exactly Severy et al. (2020). No thorough study of layouts for the notional Crescent City area has been completed, so we make no assumptions regarding layout. As discussed in Section 3.2.4, we interpolated wake losses for this area.

Table 6. Turbine quantity and layout for studied scenarios.

Farm Capacity	Turbines Quantity	Number of Rows (E-W)	Number of Columns (N-S)
48 MW	4	1	4
144 MW	12	3	4
288 MW	24	4	6
480 MW	40	5	8
1,836 MW	153	Varies	Varies

Turbines are assumed to be spaced at least seven rotor-diameters (7D) apart, following Musial et al. (2019). Based on conversations with developers, the spacing was increased to 10D in the direction of predominant winds to minimize wake effects and conflicts. Turbine rows are offset to increase the packing density while maintaining the 7Dx10D spacing (Figure 4, top view).

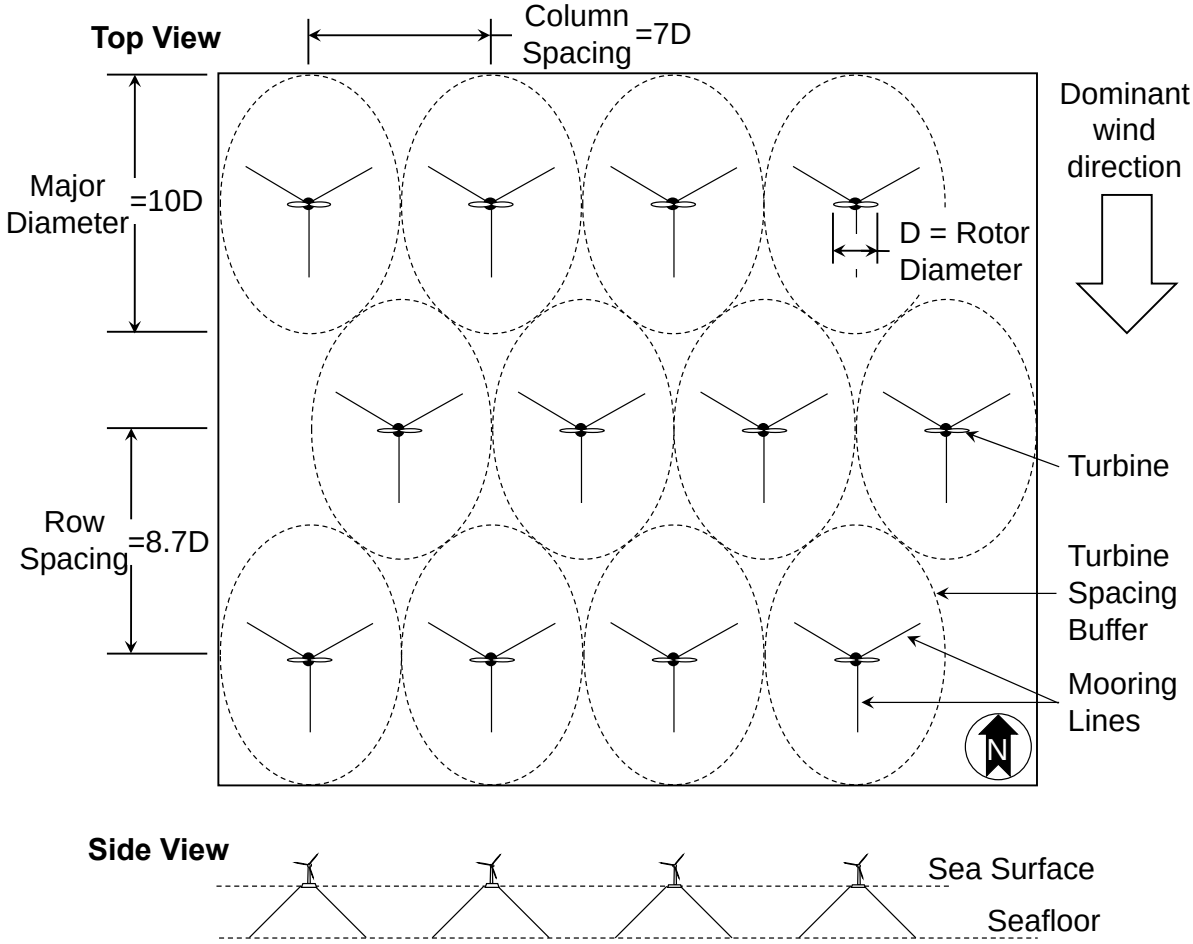

Figure 4. Turbine spacing and layout for an example 144 MW array using twelve 12 MW turbines. The top view of the array shows the horizontal spacing (top) and the side view shows the vertical profile (bottom).

3 METHODS

The analytical methods and data sources for the resource assessment are provided in this section.

3.1 Data sources

The wind speed and direction data used for this analysis is from the National Renewable Energy Laboratory's (NREL) CA20 dataset (Optis et al., 2020). Estimated wind speeds and directions are available at a variety of heights, including 140 meters above mean sea level at up to five-minute time resolution for a twenty-year period of record (i.e., 2000 through 2019). The dataset has a spatial resolution of 2 km by 2 km grid cells. In Study A, we compared the results to the previously used data, from the Wind Toolkit (NREL, n.d.), which has an 8-year period of record (i.e., 2007 through 2014).

3.2 Analysis Methods

The techniques and assumptions used to analyze the data are presented in this section.

3.2.1 Spatial Averaging

Instead of averaging wind speed values for every coordinate of data inside the area, we used the WIND Toolkit data for the coordinate closest to the centroid of each location. This was previously validated in Severy et al. (2020).

3.2.2 Adjustment of Height of Wind Speed Data

Wind speed data needed to be adjusted to the hub height[3] of the turbine (138 m) to evaluate the performance of the wind turbine. The modeled wind speed data at a height[4] of 140 m were adjusted to the hub height using the wind shear equation (Equation 1) and a constant wind shear exponent (α) of 0.1, which is typical for open waters (Masters, 2013).

$$U = U_0\left(\frac{h}{h_0}\right)^{\alpha} \qquad \textit{(Equation 1)}$$

where:

U = wind speed at height h
U_0 = wind speed at height h_0
α = wind shear exponent = 0.1
h = 138 m
h_0 = 140 m

Since h, h_0, and α are all constants, this hub height correction consistently reduced the 140 m wind speed by 0.14%. In contrast, the correction used in the earlier study to estimate the wind speed at 136 m increased the 100 m wind speed by 3.1%.

3.2.3 Power Output Calculation

The turbine power curve was used to calculate the nominal (i.e., zero losses) power output based on the modeled wind speed at 140 m adjusted to 138 m. The reference turbine power curve from NREL (Beiter et al., 2020) provided the power output at discrete points, so linear interpolation

[3] In the previous study, a turbine hub height of 136 m was used. This was preserved in the reanalysis portion of Study A.
[4] In the previous analysis, this inference was made from a height of 100 m. This is a significant source of change in our results.

between points was used to calculate the power for the exact adjusted wind speed at every available datum. In this analysis (including the reanalysis in study A), we calculated power output from the 5-minute resolution data, compared to the previous study which used hour-interval data. After calculating output at each 5-minute interval, each hour's average power was calculated. This methodology change was made to all analysis presented herein, so encompasses a small difference between what we refer to as the "previous" analysis, and the results of the previous report (i.e. Severy et al. (2020)).

3.2.4 Power Losses

All wind turbines are subject to performance losses as a result of environmental, energy management, system design, and other factors. The total turbine efficiency was determined as the sequential product of one minus each of these individual loss factors, as shown in Equation 2.

$$TE = \prod_{i=1}^{n} \left(1 - LF_i \right) \qquad \textit{(Equation 2)}$$

where:

TE = total efficiency
LF = loss factor

Two types of losses were applied to the power estimates: proportional losses and down-time (shut-off) losses. Proportional losses affect the entire system and reduce the power output proportionally due to causes such as wake effects, electrical efficiencies, and turbine performance. Down-time losses cause turbines to individually shut-off and cause the power output to be zero, due to factors such as curtailment, high wind control hysteresis, and site access limitations.

Most of the loss factor values were either industry values obtained from AWS Truepower (2014), or literature values from Musial, Beiter, et al. (2019), or Musial, Heimiller, et al. (2016). Wake effect losses were modeled using the Eddy-Viscosity method (as recommended in Churchfield (2013)) and were calculated using NREL's System Advisor Model (SAM), Beta Version 2020.11.29. Power loss due to wake effects was modeled at the centroid, for the median-power year in the period of record (see Figure 18) at each location.

The combined effect of proportional losses before wake effects, and shut-off losses, were 6.4% and 7.3%, respectively (see list of all loss factors in Appendix B).

To model the shut-off losses, the power output for the entire farm was set to zero at 7.3% of times throughout the year, selected at random. The random application of these losses should best represent the unexpected nature of failures and grid outages. After shut-off losses were applied, power output at all hours was reduced by the 6.4% proportional losses (such as efficiency losses) along with the site-specific wake loss factors (Table 7).

Table 7. Power loss factors due to wake losses. Wake losses change based on location and wind farm scale.

Wind Farm Size	Humboldt Call Area & Study Area	Cape Mendocino	Crescent City
48 MW	0.08%	0.01%	0.04%
144 MW	0.84%	0.82%	0.92%
288 MW	1.15%	1.04%	1.20%
480 MW	1.37%	1.23%	1.42%
1836 MW	1.79%	1.52%	1.81%[a]

In the previous analysis, a binomial distribution was used to set each time interval's (i.e. hour's) power to zero with probability 7.3%. This meant that, in practice, some years received more shutoffs than others. In the new analysis, 7.3% of shutoff time periods were randomly ordered, then applied to every year. The result is that every year has precisely the same frequency (and temporal location) of shutoffs. This methodology change was made to all analysis presented herein, so encompasses a small difference between what we refer to as the "previous" analysis, and the results of the previous report (i.e. Severy et al. (2020)).

The resulting losses from all factors ranged from 13.1%[5] for a 48 MW wind farm in the notional Cape Mendocino area to 14.7% for an 1,836 MW Humboldt Call Area or notional Crescent City area wind farm (14.4% for a notional Cape Mendocino farm). Beiter et al. (2020) calculated total losses of 14.6% to 14.8% for Humboldt wind farms with commercial operation dates of 2032 and 2027, respectively, 13.8% to 14.0% for notional Cape Mendocino farms, and 14.5% to 14.7% for Del Norte (the Crescent City region) wind farms with the same commercial operation dates, all quite close to our loss factors for 1,836 MW farms.

3.2.5 Calculation of Confidence and Tolerance Intervals

A confidence interval describes how confidently we know the value of a population parameter. For example, in the long run we would expect that 95 out of 100 calculated 95% confidence intervals of sample average annual energy production to contain the true population average annual energy production. A confidence interval for the population mean is calculated as shown in Equation 3:

[5] This number is slightly smaller than the losses calculated in Appendix B due to the randomness in when shutdowns occur.

$$CI = \bar{x} \pm t\left(\frac{\alpha}{2}, n-1\right) * \frac{sd}{\sqrt{n}} \qquad \textit{(Equation 3)}$$

Where:

CI = confidence interval
$\bar{x}$ = sample mean
sd = sample standard deviation
n = number of observations
α = probability of a sample falling outside the confidence interval; for a 95% confidence interval, $\alpha = 0.05$
t = critical value of the *t* distribution, a function of $\alpha/2$ and *n-1*. *t* = 2.093 for a 95% confidence interval with and *n* = 20 observation (years).

Tolerance intervals describe the range over which *k%* of future observations would be expected to fall, with a confidence level of (1 - α)%. They are calculated according to Equation 4:

$$TI = \bar{x} \pm C(k, 1-\alpha, n) * sd \qquad \textit{(Equation 4)}$$

Where:

TI = tolerance interval
$\bar{x}$ = sample mean
sd = sample standard deviation
n = number of observations
C = tolerance critical value: 2.752 for *k* = 95%, (1 - α) = 95% and *n* = 20.

The methods used to calculate tolerance intervals and confidence intervals rely on the assumption that underlying data (annual capacity factor and generation) are normally distributed. The quantile-quantile plots shown in Appendix C for the capacity factors of 144 MW developments support the assumption of normality for annual capacity factors and annual generation. Annual generation and annual capacity factors for the 144 MW and other farm sizes are linear functions of these data for 144-MW installations and so have the same normality properties. Note that for the notional Cape Mendocino area, high annual capacity factors are overrepresented compared to a normal distribution, so more than 2.5% of future observations are likely to fall above the presented 95% tolerance intervals.

4 RESULTS

The results from the resource assessment include analyses of wind speed and power generation patterns. We begin with the results of Study A, and then present the results for Studies B and C.

4.1 Study A Results

This study documents differences between the old and new analyses for scenarios generated for the Humboldt Call Area (48 MW, 144 MW, 1,836 MW) and the notional Cape Mendocino area (144 MW, 1,836 MW). These differences come from two primary sources: First, the new datasets make different predictions regarding the relative frequency distribution of wind speeds. Second, rather than extrapolate wind speed to the assumed rotor height from 100 m, as was done in the previous analysis, we extrapolated from data at a height of 140 m. Previously, speed was

extrapolated from 100 m to 136 m; in the new analysis, wind speed is extrapolated to 138 m (reflecting updated turbine hub heights from Beiter et al. (2020)) from 140 m. Adjustments to the turbine power curve play a smaller role in the power generation (Section 4.1.3).

4.1.1 Wind Speed Distribution

Comparison of the resulting empirical cumulative distribution functions (eCDFs) of 5-minute interval wind speeds for both sites using the previous and new analysis methods are shown in Figure 5. Both new curves are shifted to the right, toward higher wind speeds relative to the old curves. The new analysis predicts a higher top-end speed distribution, with eCDFs diverging near 10 meters per second and 15 meters per second for the Humboldt Call Area and the notional Cape Mendocino area, respectively. The notional Cape Mendocino area provides higher wind speeds than the Humboldt Call Area by both analyses.

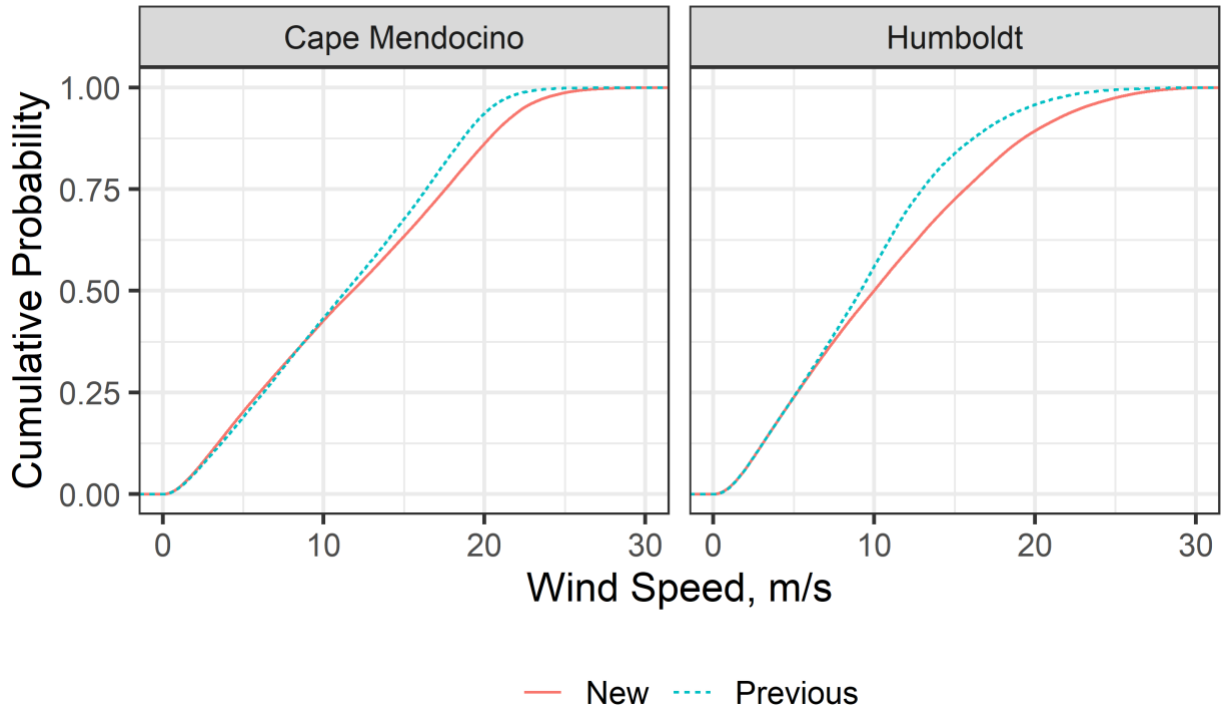

Figure 5. Comparison of previous and new cumulative probability distribution functions of wind speed in both locations. Wind speeds are at the turbine hub heights, 136-m for the previous analysis and 138-m for the new analysis.

The histograms of wind speed (Figure 6) show the continuous frequency of occurrence of each wind speed. In the previous analysis, the Humboldt Call Area had a noticeable Weibull distribution, which is common for wind regimes, with the most frequent wind speed being 10 meters per second (at a height of 136 m) and a long tail of high wind speeds at lower probability. In the new analysis, the wind speed at the Humboldt Call Area is most frequently near 2.5 meters per second (at a height of 138 m). The notional Cape Mendocino area wind speed profile has nearly uniform probability of occurrence between 3 meters per second and 17 meters per second in both the previous and the new analysis, though the upper end is stretched further in the new analysis, to 20 meters per second.

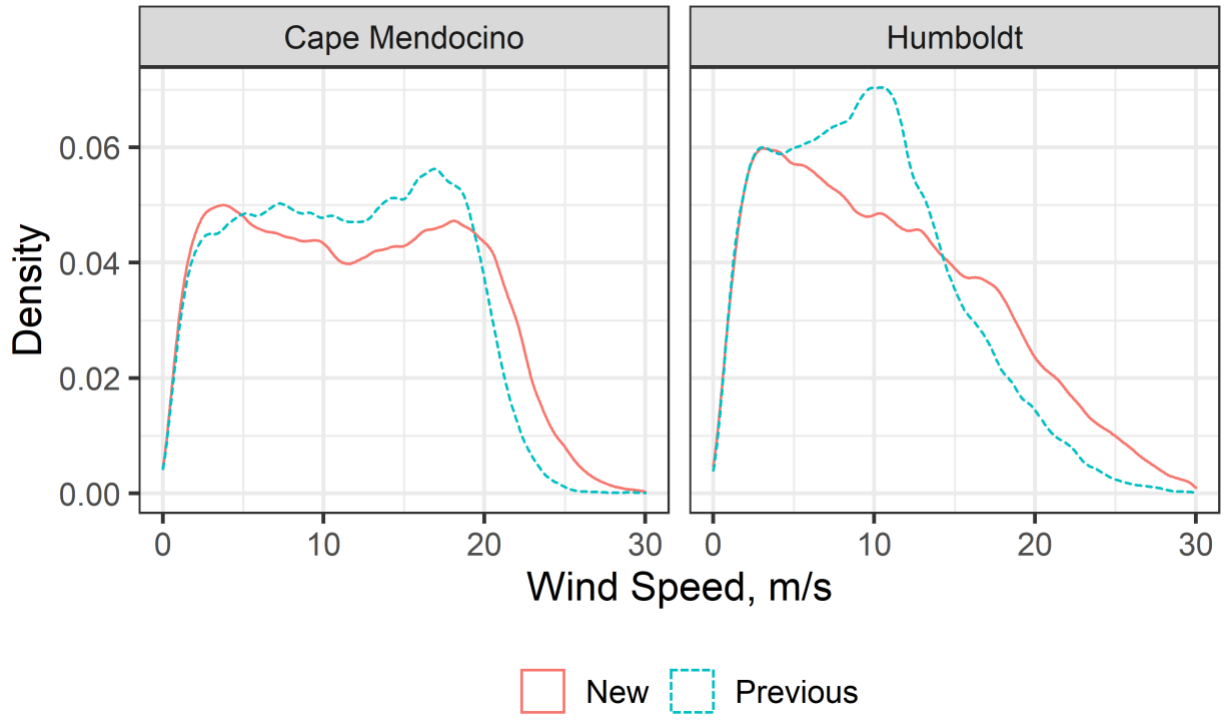

Figure 6. Density function of wind speeds for the Humboldt Call Area (right) and the notional Cape Mendocino area (left). The hump of high probabilities around 10 meters per second in the old model has vanished in the new modeling. Wind speeds are at the turbine hub heights, 136-m for the previous analysis and 138-m for the new analysis.

The distribution of wind speed varies by season (Figure 7) in both the new and old analysis. For all seasons in the Humboldt Call Area, the distributions are consistently shifted to the right toward higher speeds compared to the previous analysis. The greatest change in the new analysis for the Humboldt Call Area comes during summer, while spring shows the least change. The values for the notional Cape Mendocino area have hardly changed at all, though the largest change again comes during summer.

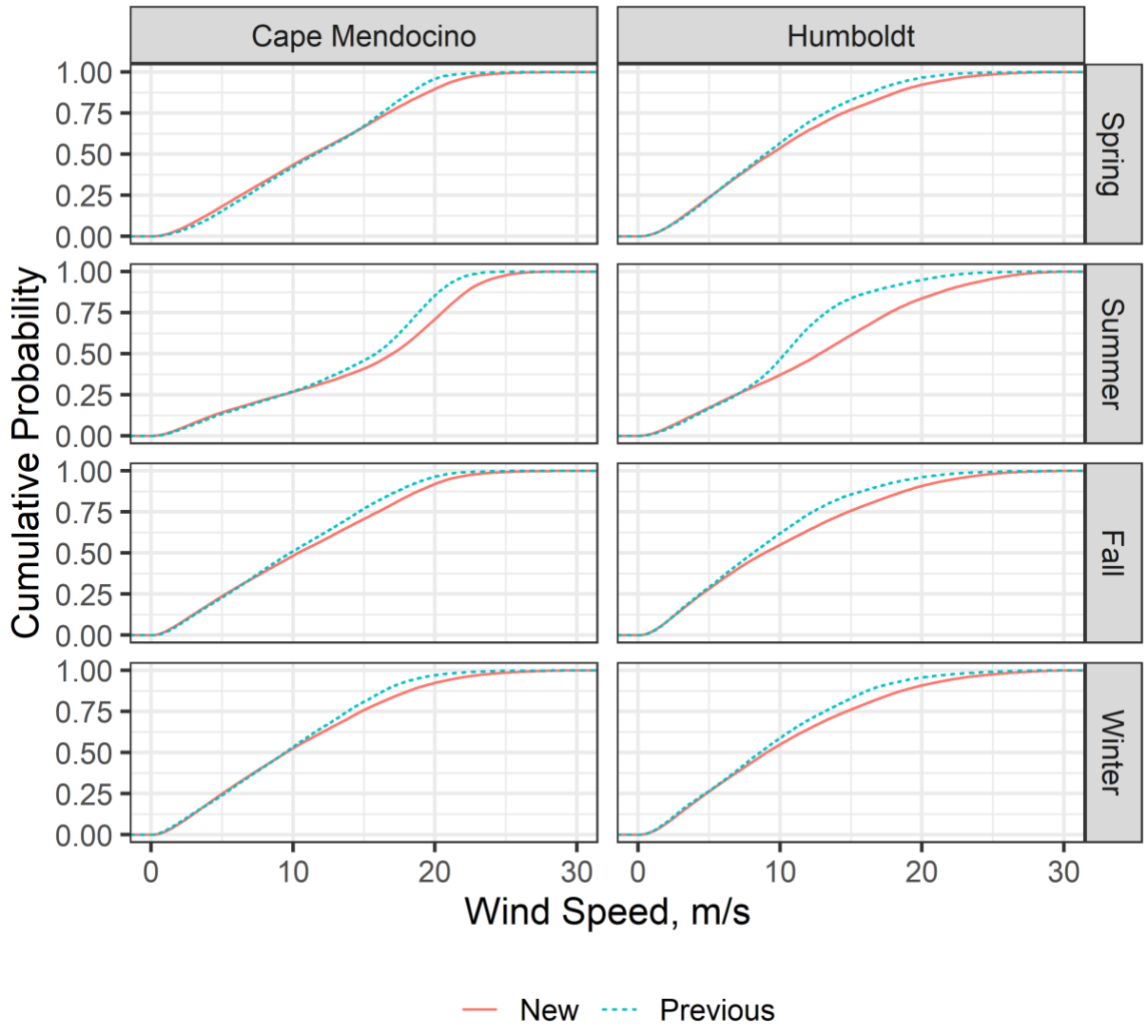

Figure 7. Cumulative distribution function of wind speed by season at both locations. Wind speeds are at the turbine hub heights, 136-m for the previous analysis and 138-m for the new analysis. Each season is three months, with spring beginning in March.

4.1.2 Wind Direction

Based on the new wind speed data, wind roses from the Humboldt Call Area (Figure 8), the notional Cape Mendocino area (Figure 9) show a consistent bi-directional wind pattern with predominant winds from the north. This trend was observed in the previous analysis at the Humboldt Call Area and the notional Cape Mendocino area. The wind roses below separate the wind speeds into four categories, based on the power curve of the turbine:

- Below cut in speed: 0 to 3 m/s; no power output because wind turbine is not spinning.
- Increasing power output: 3 to 11 m/s; power output increases with wind speed.
- Rated wind speed: 11 to 30 m/s: power production is constant at rated power output.
- Above cut out speed: 30 + m/s; no power output because wind speed is too high.

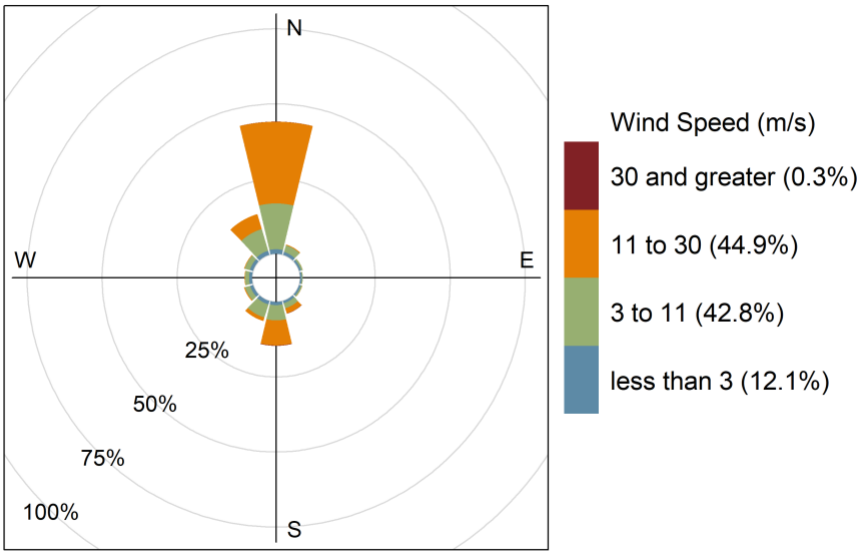

Figure 8. Annual wind rose for the Humboldt Call Area. Percentages on the radial axis represent the percent of time the wind speeds occurred.

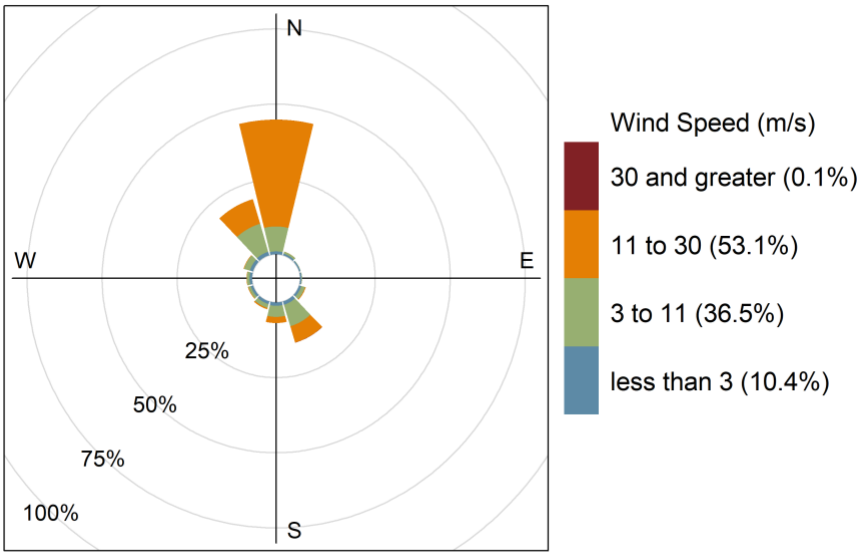

Figure 9. Annual wind rose for the notional Cape Mendocino area. Percentages on the radial axis represent the percent of time the wind speeds occurred.

4.1.3 Power Generation

Power generation profiles for the different wind farm scenarios were calculated after applying all loss factors (see Appendix B). Table 8 summarizes annual energy production two ways: First, the confidence intervals describe the precision of estimating the true annual mean, and second, the tolerance intervals describe where future values of annual mean energy production are likely to occur. For example, in 95% of future years, a 48-MW development at the Humboldt Call Area

centroid is expected to produce between 187 and 251 GWh of energy according to the new model.

Table 8. Annual energy production (AEP) summary for Study A wind farm scenarios. The previous model uses WIND Toolkit data, and infers power at 136 m from wind speed data at 100 m. The new model uses the CA20 dataset and new turbine curve and wake losses, and infers power at 138 m from wind speed data at 140 m. The new model draws from a sample of 20 years for wind speed data, whereas the previous model uses a sample of 8 years.

Region	Size (MW)	AEP 95% Confidence Interval, CA20 (GWh per year)	AEP 95% Confidence Interval, WIND Toolkit (GWh per year)	AEP 95% Tolerance Interval, CA20 (GWh per year)	AEP 95% Tolerance Interval, WIND Toolkit (GWh per year)
Humboldt	48	219 ± 5.47	208 ± 9.88	187 to 251	175 to 240
Cape Mendocino	144	719 ± 16	722 ± 11.3	625 to 814	685 to 759
Humboldt	144	652 ± 16.3	616 ± 29.3	556 to 747	520 to 713
Cape Mendocino	1836	9,110 ± 203	9,140 ± 143	7,910 to 10,300	8,670 to 9,610
Humboldt	1836	8,230 ± 206	7,750 ± 369	7,020 to 9,440	6,540 to 8,960

These data display several significant trends. First, predicted energy production for the Humboldt Call Area increases by 6%, and the precision of the estimate increases (narrower confidence interval) due to the larger sample (20 years, versus the previous eight years). The coefficient of variation (the standard deviation divided by the mean) is 5.0% in the new model, about half of the 9.5% in the previous model. The width of the tolerance remains about the same, indicating the newer model does not predict higher year-to-year variation. Second, both observations are reversed for the notional Cape Mendocino area: Energy production is not higher with the new model, and the width of the confidence interval actually increases, despite the larger *n* (years of observation), with the coefficient of variation increasing from 3.1% to 4.4%. This conclusion can again be observed in the tolerance interval, which this time has greater width. Third, the notional Cape Mendocino area continues to have higher predicted generation, though the gap has narrowed significantly.

The capacity factors shown in Table 9 were calculated by dividing the total energy production by the theoretical maximum energy production: the nameplate capacity times 8760 hours per year. In the new model, the Humboldt Call Area's average annual capacity factor ranges from 51 to 52%, while in the previous model it was significantly lower: 48 to 49%. For the notional Cape Mendocino area, on the other hand, the capacity factor values remain essentially unchanged at 57%. The capacity factors of larger wind farms are slightly lower than smaller wind farms due to increased wake effects within larger turbine arrays. These, and other trends, are consistent with the analysis of annual energy production because capacity factor and total production are linearly scaled.

Table 9. Capacity factor (CF) summary for Study A wind farm scenarios. The previous model uses WIND Toolkit data, and infers power at 136 m from wind speed data at 100 m. The new model uses the CA20 dataset and new turbine curve and wake losses, and infers power at 138 m from wind speed data at 140 m. The new model draws from a sample of 20 years for wind speed data, whereas the previous model uses a sample of 8 years.

Region	Size (MW)	CF 95% Confidence Interval, CA20	CF 95% Confidence Interval, WIND Toolkit	CF 95% Tolerance Interval, CA20	CF 95% Tolerance Interval, WIND Toolkit
Humboldt	48	0.521 ± 0.013	0.494 ± 0.023	0.444 to 0.597	0.416 to 0.571
Cape Mendocino	144	0.570 ± 0.013	0.572 ± 0.009	0.495 to 0.645	0.543 to 0.602
Humboldt	144	0.517 ± 0.013	0.488 ± 0.023	0.441 to 0.593	0.412 to 0.565
Cape Mendocino	1836	0.566 ± 0.013	0.568 ± 0.009	0.492 to 0.640	0.539 to 0.597
Humboldt	1836	0.512 ± 0.013	0.482 ± 0.023	0.437 to 0.587	0.406 to 0.557

The annual energy production and capacity factor provide a description of how the wind turbine arrays will perform when summed across the whole year. A generation duration curve is used to investigate how the level of power production varies throughout the year. The generation duration curves for the Humboldt Call Area and the notional Cape Mendocino area show the power output on the vertical axis and the cumulative number of hours per year when the wind farm is operating at that power output or above on the horizontal axis (Figure 10). For all scenarios, the wind farms are often operating at their maximum capacity or at zero power output, as shown in the horizontal portions of the lines on the left and right of the plots, respectively. Note that, in the new model, arrays in the Humboldt Call Area are predicted to produce full output a larger fraction of the time, while the result for the notional Cape Mendocino area remains largely unchanged. The amount of time operating at the maximum power output corresponds to the amount of time that the wind speed is in the turbine's rated wind speed range from 11 to 30 meters per second (11 to 25 meters per second in the previous model). The amount of time that the wind farm is at zero power output corresponds to times when the wind speed is less than 3 meters per second or the turbines are at 0 MW output based on the shutoff loss factors described in Section 3.2.4.

For all scenarios, the most striking feature of the generation duration curves is that they produce either full power or no power for over 50% of the year; during the remaining time, power output for each turbine is between 0 and 12 MW.

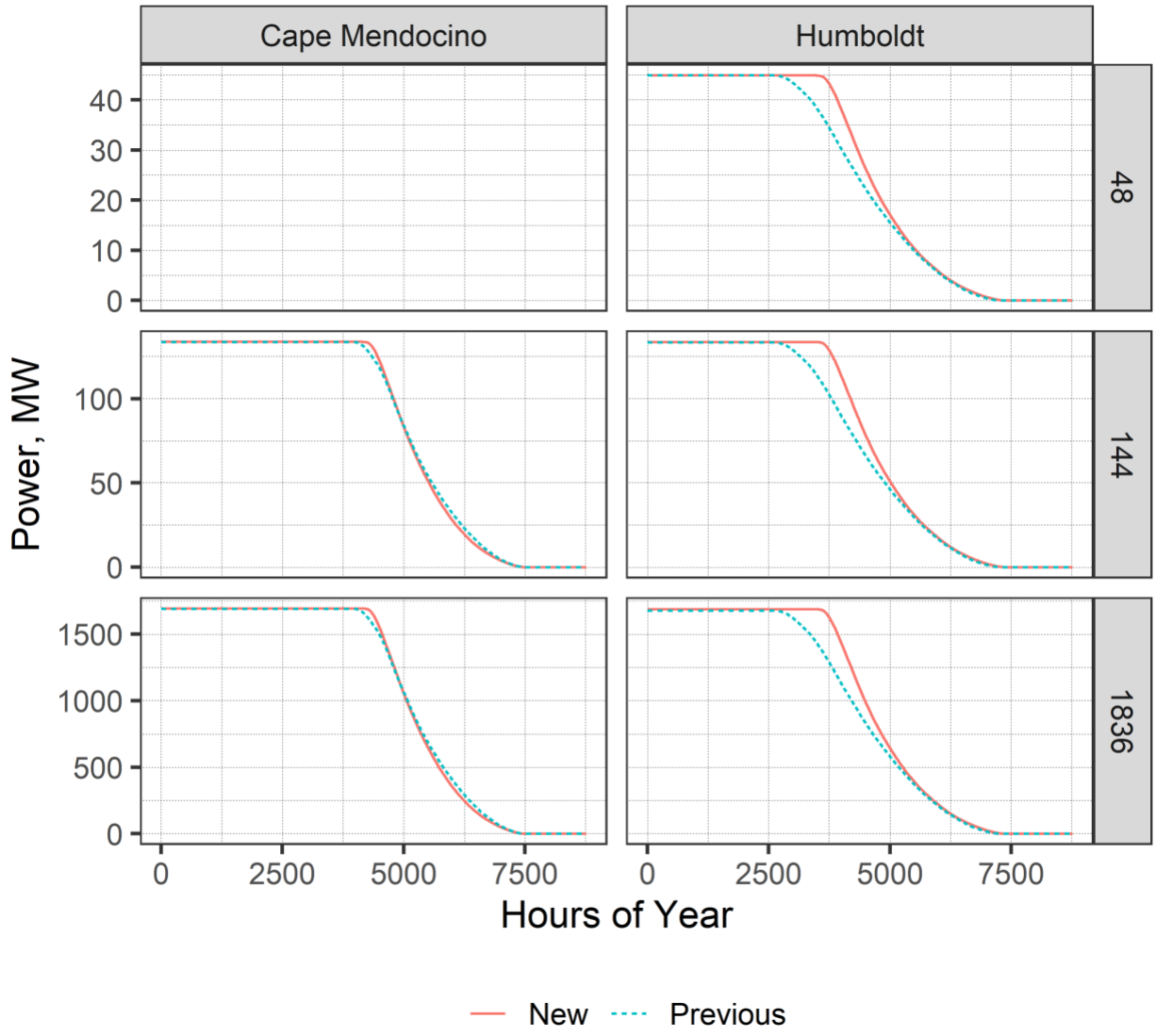

Figure 10. Generation duration curves for all project scenarios. Cape Mendocino at 48 MW is blank because it was not studied. Note the difference in power scales between the rows of graphs.

4.2 Study B Results

This section presents the results of Study B, which provides the power estimates required for Task 2.1 and analyzes the wind farm performance at the three locations within the Humboldt Call Area at scales of 48 MW, 144 MW, 288 MW, and 480 MW. The study compares wind farm performance at the centroid of the entire Humboldt Call Area to performance at two additional locations: the centroids of 480 MW developments inside the farm, but adjacent to the eastern and western edges, as shown in Figure 11.

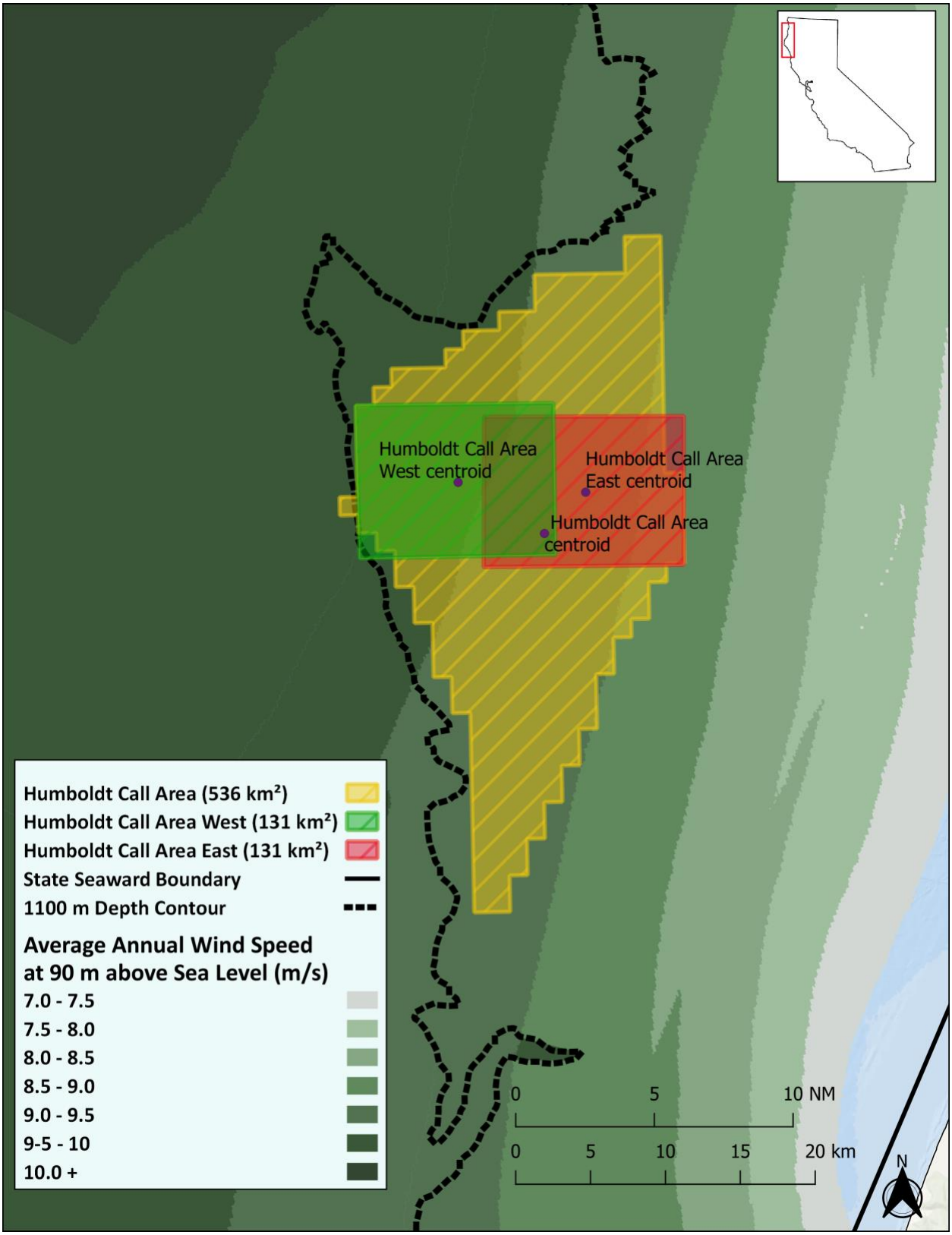

Figure 11. The Humboldt Call Area and notional subregions, with their centroids depicted as purple dots.

4.2.1 Wind Speed Distribution

Figure 12 shows the cumulative distribution function of wind speeds for each of the three locations. Unsurprisingly, the wind speeds increase moving from east to west across the call area, but the changes appear to be relatively small. For example, the difference in the 75th percentile of the wind speeds between the east and west locations is only 0.58 meters per second or 3.7%.

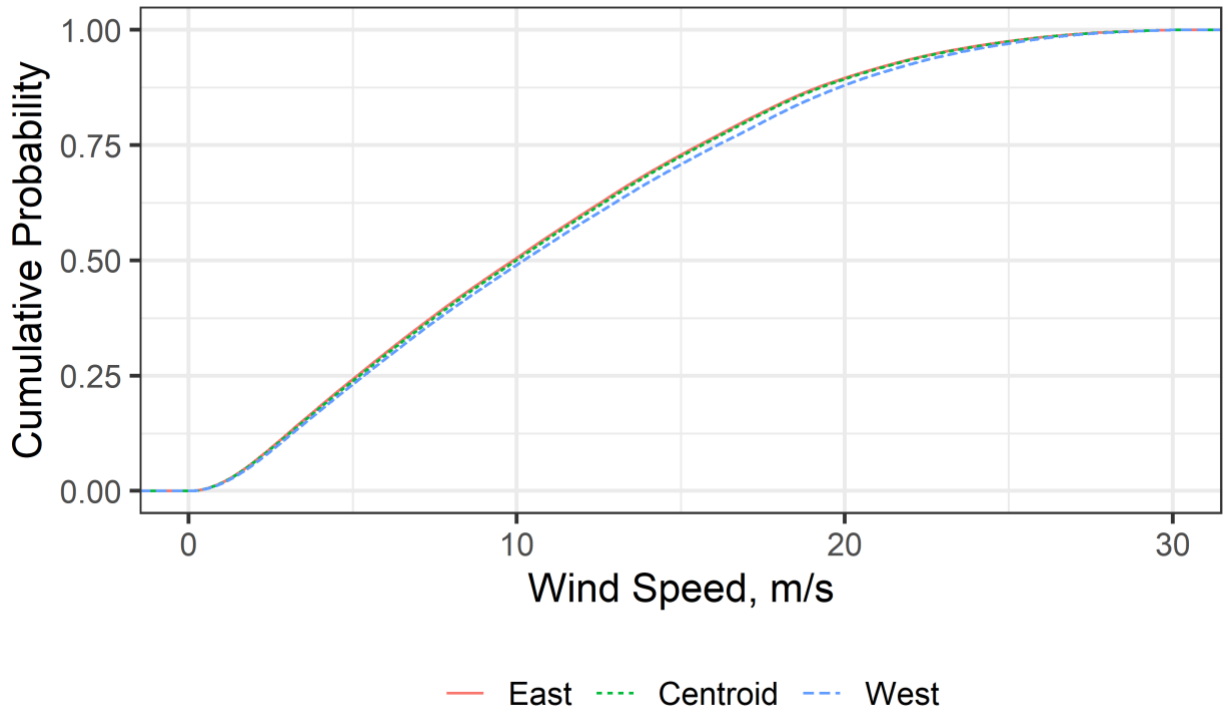

Figure 12. Cumulative distribution function of wind speed in the three Humboldt Call Area locations at a turbine hub height of 138 m.

4.2.2 Power Generation

Power generation profiles for the different wind farm scenarios were calculated after applying all loss factors shown in Appendix B. Table 10 summarizes annual energy production two ways: first, confidence intervals describe the precision of estimating of the true annual mean, and second, tolerance intervals describe where future values of annual mean energy production are likely to occur.

Differences are relatively small, with only a 2% difference in power production between the east and west locations.

Table 10. Annual energy production (AEP) summary for Study B wind farm scenarios (Humboldt Call Area) according to the new model with n = 20 years.

Location	Size (MW)	AEP 95% Confidence Interval (GWh per year)	AEP 95% Tolerance Interval (GWh per year)
East	48	217 +/- 5.47	185 to 250
Centroid	48	219 +/- 5.47	187 to 251
West	48	222 +/- 5.3	191 to 253
East	144	647 +/- 16.3	552 to 743
Centroid	144	652 +/- 16.3	556 to 747
West	144	662 +/- 15.8	569 to 754
East	288	1,290 +/- 32.5	1,100 to 1,480
Centroid	288	1,300 +/- 32.5	1,110 to 1,490
West	288	1,320 +/- 31.5	1,130 to 1,500
East	480	2,150 +/- 54	1,830 to 2,460
Centroid	480	2,160 +/- 54	1,840 to 2,480
West	480	2,190 +/- 52.3	1,890 to 2,500

The capacity factors in Table 11 were calculated by dividing the total annual energy production by the theoretical maximum energy production: the nameplate capacity times 8760 hours per year. Capacity factors increase by about 1% from east to west, e.g., from 51.7% to 52.9% for the 48-MW size farm.

Table 11. Capacity factor (CF) summary for Study B wind farm scenarios (Humboldt Call Area) according to the new model with n = 20 years.

Location	Size (MW)	CF 95% Confidence Interval	CF 95% Tolerance Interval
East	48	0.517 +/- 0.013	0.441 to 0.594
Centroid	48	0.521 +/- 0.013	0.444 to 0.597
West	48	0.529 +/- 0.013	0.454 to 0.603
East	144	0.513 +/- 0.013	0.437 to 0.589
Centroid	144	0.517 +/- 0.013	0.441 to 0.593
West	144	0.525 +/- 0.013	0.451 to 0.598
East	288	0.512 +/- 0.013	0.436 to 0.587
Centroid	288	0.515 +/- 0.013	0.439 to 0.591
West	288	0.523 +/- 0.012	0.450 to 0.596
East	480	0.510 +/- 0.013	0.435 to 0.586
Centroid	480	0.514 +/- 0.013	0.438 to 0.589
West	480	0.522 +/- 0.012	0.449 to 0.595

Like the wind speed distribution, generation duration curves are practically indistinguishable across the three locations. While output is zero for the same amount of time regardless of location, more westerly locations produce full power for more hours of the year.

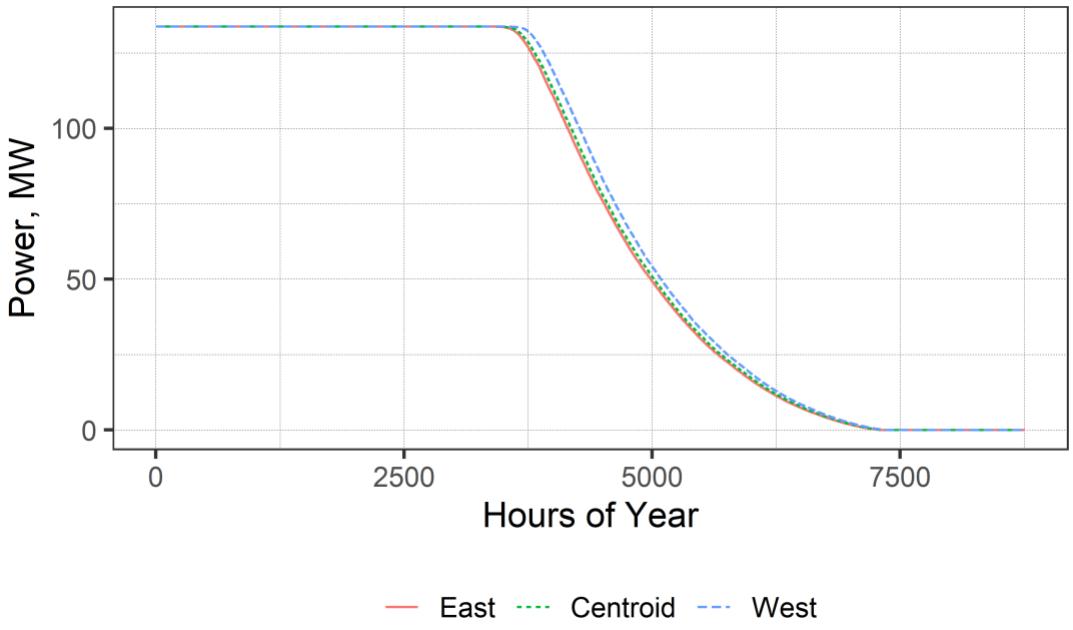

Figure 13. Generation duration curve comparison for the three Humboldt Call Area locations, shown at the scale of 144 MW.

4.3 Study C Results

In Study C, we compare performance of wind farms located at the centroids of all three areas (Humboldt Call Area, notional Cape Mendocino area, and notional Crescent City area) at all five studied sizes, as well as a comparison to a hypothetical research area located just outside of the eastern edge of the Humboldt Call Area at 48-MW scale (called the Humboldt Study Area).

4.3.1 Wind Speed Distribution

Figure 14 shows the cumulative distribution function of wind speeds at the four locations. The notional Crescent City area and the notional Cape Mendocino areas consistently provide higher wind speeds than the Humboldt Call Area. While the notional Cape Mendocino area provides the greatest frequency of moderate speeds, the Crescent City area provides the highest frequency of winds above 20 meters per second. Finally, the notional Humboldt Study Area provides the lowest speeds.

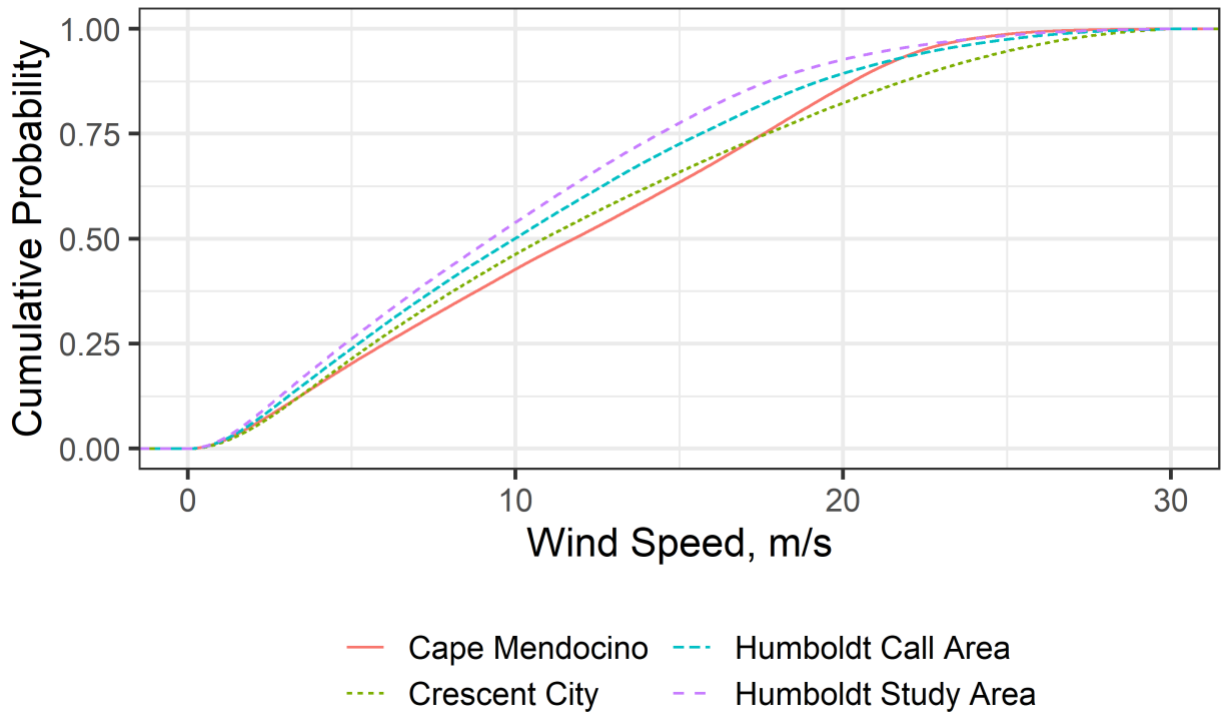

Figure 14. Cumulative probability distribution function of wind speed in the four regions at the 138-m turbine hub height.

Histograms of wind speed (Figure 15) show the frequency of occurrence of wind speed, using a bin width of 1 meter per second. Here, too, one can observe the frequent occurrence of moderate wind speeds in the notional Cape Mendocino area, and the relatively heavy tail of high wind speeds in the notional Crescent City area.

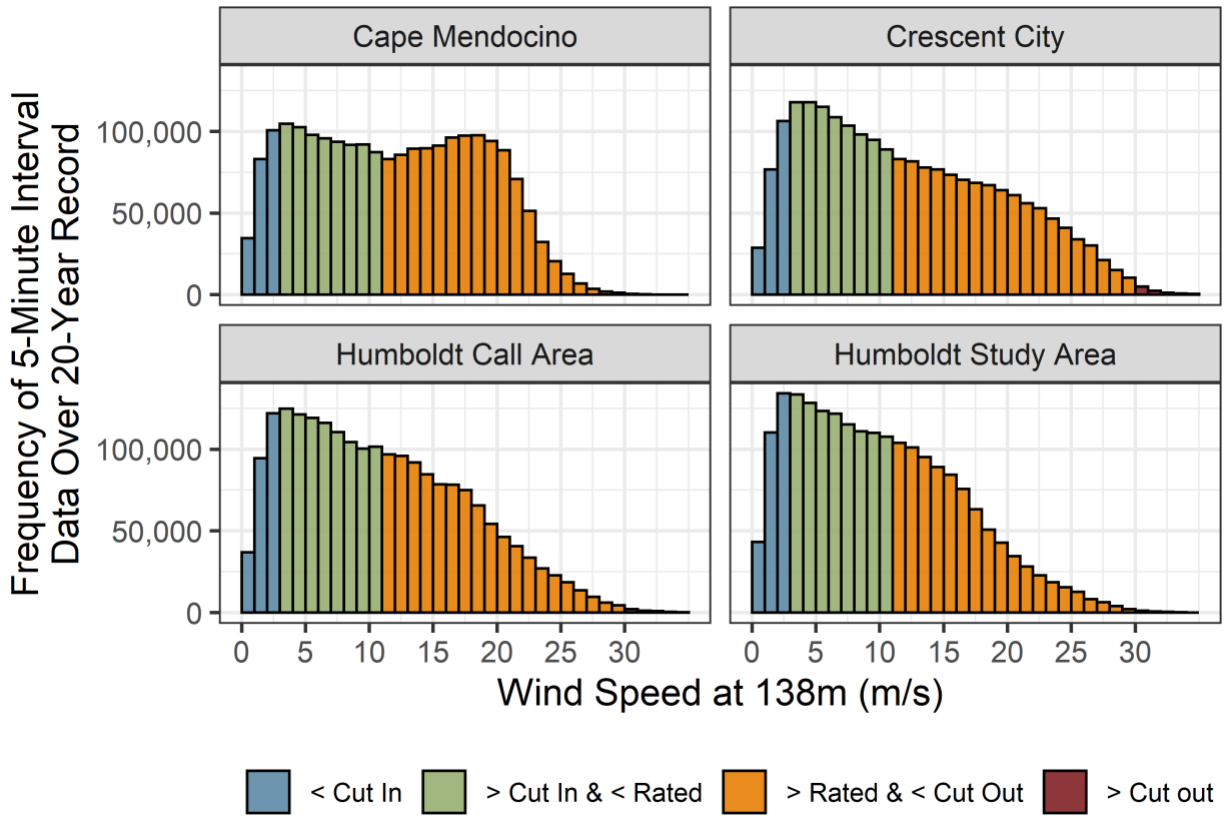

Figure 15. Histograms of wind speed and frequency of occurrence for notional Cape Mendocino area (top left), notional Crescent City area (top right), the Humboldt Call Area (bottom left), and the notional Humboldt Study Area (bottom right). The y-axis is frequency of occurrence for 5-minute intervals in the 20-year period of record binned into 1 meter per second bins. Wind speed is measured at the 138-m turbine hub height.

The distribution of wind speed varies by season (Figure 16) and location, with all sites showing higher wind speeds in the summer months than in the winter months. The Humboldt Call Area and notional Humboldt Study Area have the least seasonal variation, which may be a desirable feature depending on the seasonality of the load shape being served.

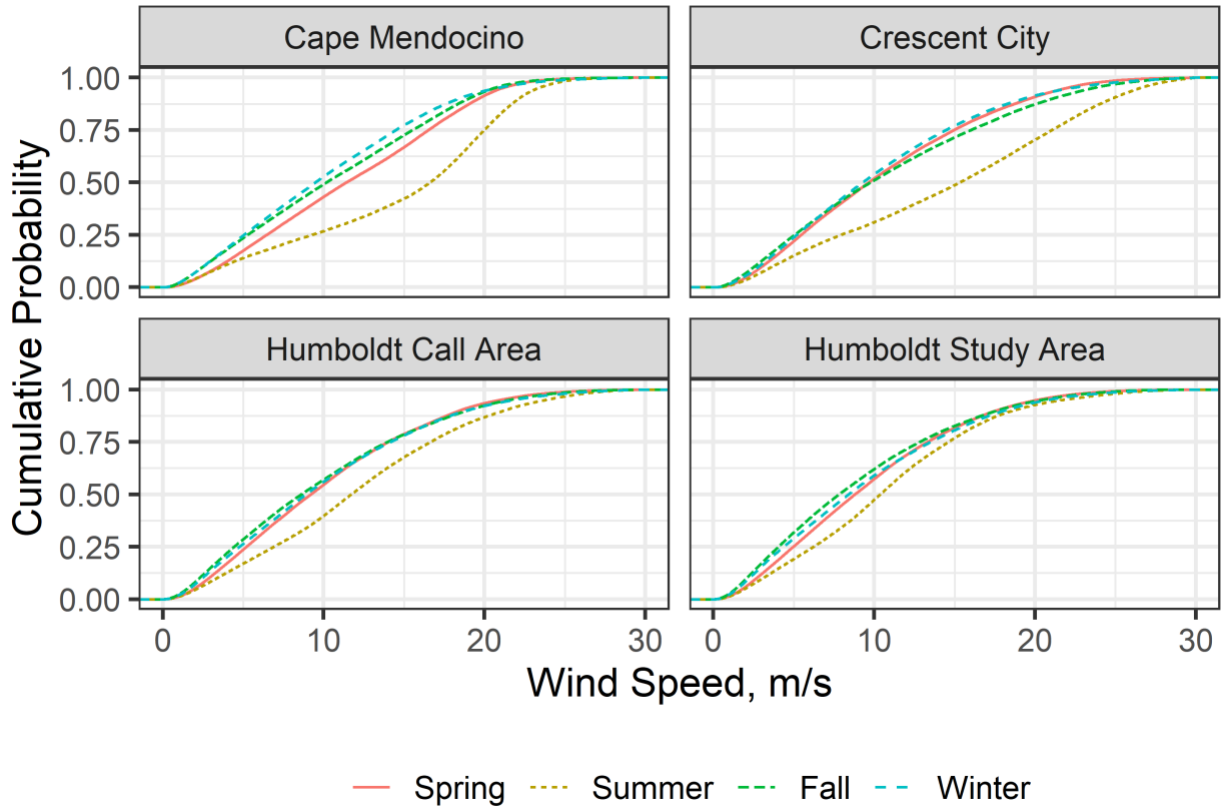

Figure 16. Cumulative distribution function of 138-m wind speed by season at the four Study C locations: A notional Cape Mendocino area (top left), a notional Crescent City area (top right), the Humboldt Call Area (bottom left), and a notional Humboldt Study Area (bottom right). Each season is three months, with spring beginning in March.

4.3.2 Wind Direction

The wind rose for the notional Crescent City area (Figure 17) shows a consistent bi-directional wind pattern with predominant winds from the north. This trend was observed in the Humboldt Call Area and the notional Cape Mendocino area. The wind rose separates the wind speeds into four categories, based on the power curve of the turbine:

- Below cut in speed: 0 to 3 m/s; no power output because wind turbine is not spinning.
- Increasing power output: 3 to 11 m/s; power output increases with wind speed.
- Rated wind speed: 11 to 30 m/s: power production is constant at rated power output.
- Above cut out speed: 30 + m/s; no power output because wind speed is too high.

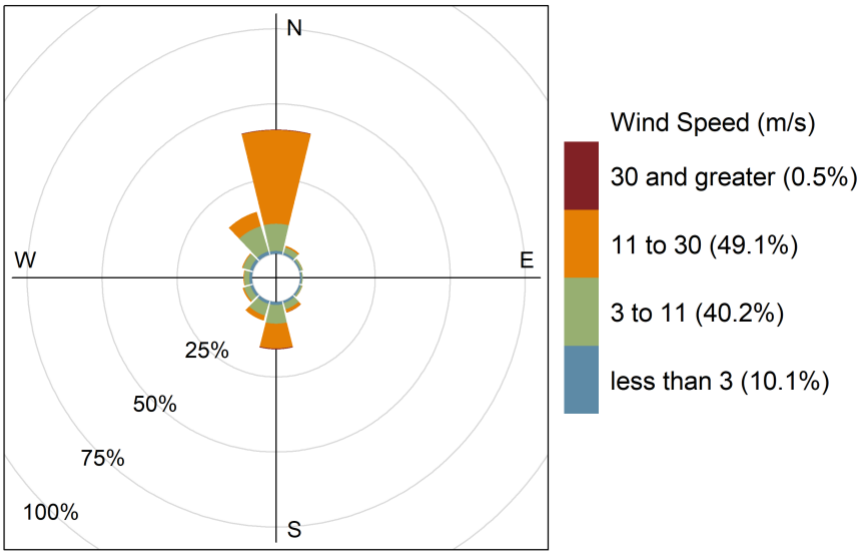

Figure 17. Annual wind rose for the notional Crescent City area. Percentages on the radial axis represent the percent of time the wind speeds occurred.

4.3.3 Wind Speed Variability

This section looks at the variability of wind speed from between years, seasons, and hour of day across the three centroidal locations. Since the two Humboldt locations are so similar, the notional Humboldt Study Area location is not discussed herein. From the twenty-year period of modeled data, the annual median wind speed varied among years by about 2 meters per second. Since there are an even number of years, there were two median years for each location, which tended to cluster tightly around two periods, as shown in Figure 18. These are 2007 and 2013 for the notional Cape Mendocino area, 2008 and 2013 for the notional Crescent City area, and 2009 and 2014 for the Humboldt Call Area. For each location, we chose one year: 2013 for the notional Crescent City and Cape Mendocino areas, and 2014 for the Humboldt Call Area. These median years are used in analysis below.

Note that for all years, the annual median wind speed in the Humboldt Call Area is lower than in the other two areas, and the speeds in the notional Crescent City area are lower than in the notional Cape Mendocino area in 16 of the 20 years.

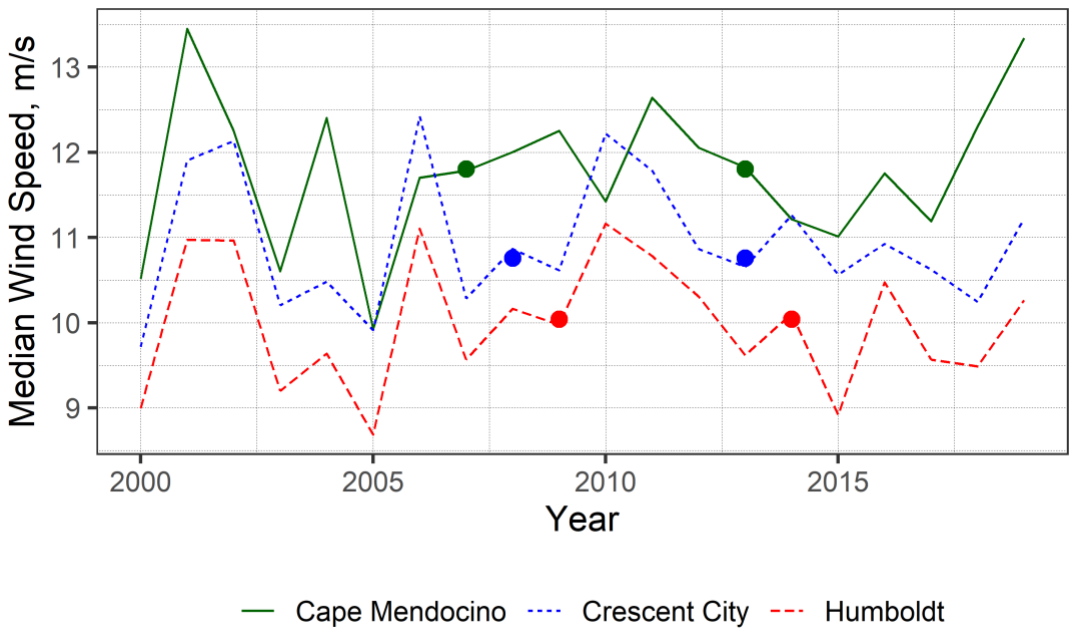

Figure 18. Results of median wind speed year analysis for the centroids of the three investigated regions. Note the y-axis does not include 0 meters per second. Dots indicate the median years and median wind speed at 138 m.

There is, visually, a significant degree of correlation across the sites, which is explored explicitly in Figure 19. The degree of correlation between the Humboldt Call Area and the notional Crescent City area is remarkable, and, while the correlation between the notional Cape Mendocino area and the Humboldt Call Area is noisier, it is still strong.

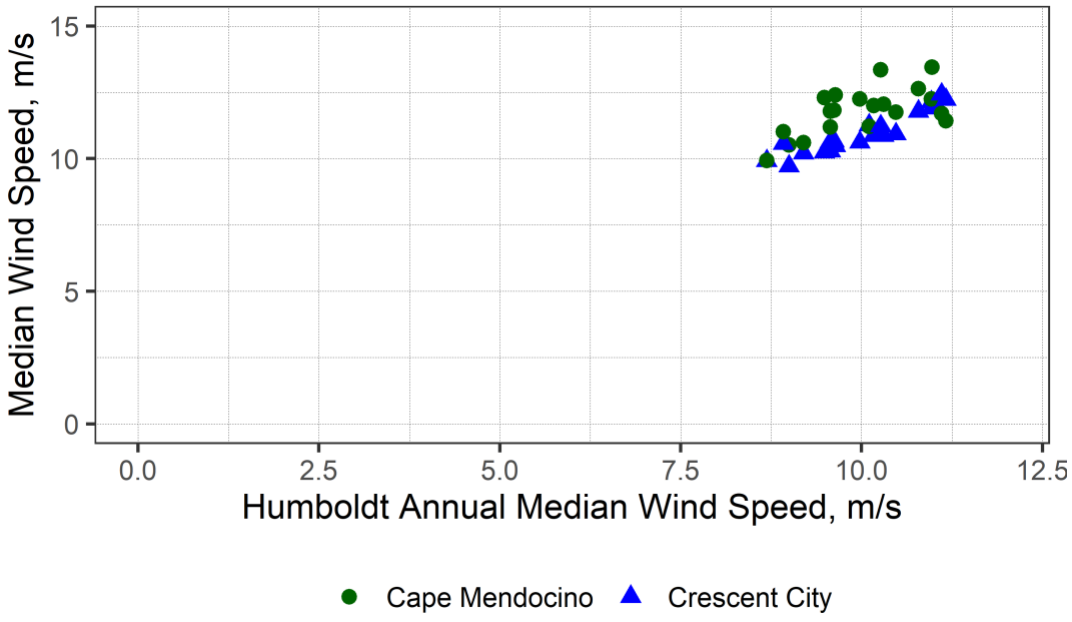

Figure 19. Correlation between wind speed at the Humboldt Call Area Centroid and the notional Cape Mendocino and Crescent City areas at 138 meters.

Daily profiles of wind speed show very little variation on average. On average, throughout the year, the Humboldt Call Area receives the lowest wind speed between noon and six pm (Figure 20), though this variation is less than 1 meters per second. The average over the period of record is quite similar to the median year for this site.

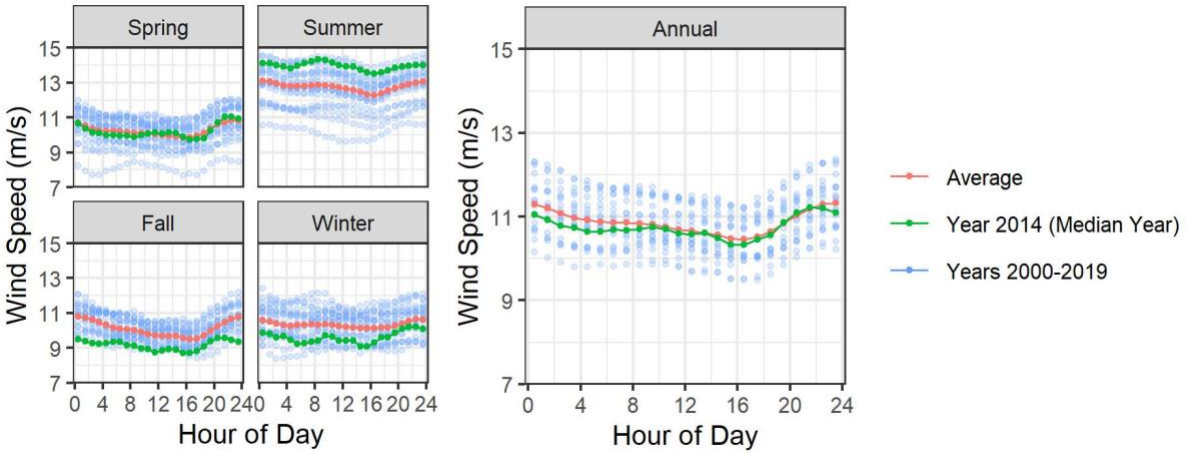

Figure 20. Daily profile of average wind speed at 138 m for the year (right) and by season (left) for the Humboldt Call Area. The dots represent data averaged for each of the seven years with the average and median years highlighted in red and green, respectively. Note that the annual average plot does not have the same axis limits as the individual seasonal plots.

The daily profile at the notional Cape Mendocino area, shown in Figure 21, shows a similar daily trend to Humboldt with apparently flat daily generation profiles in spring and winter, but more variability on summer. The average is again strikingly similar to the median year.

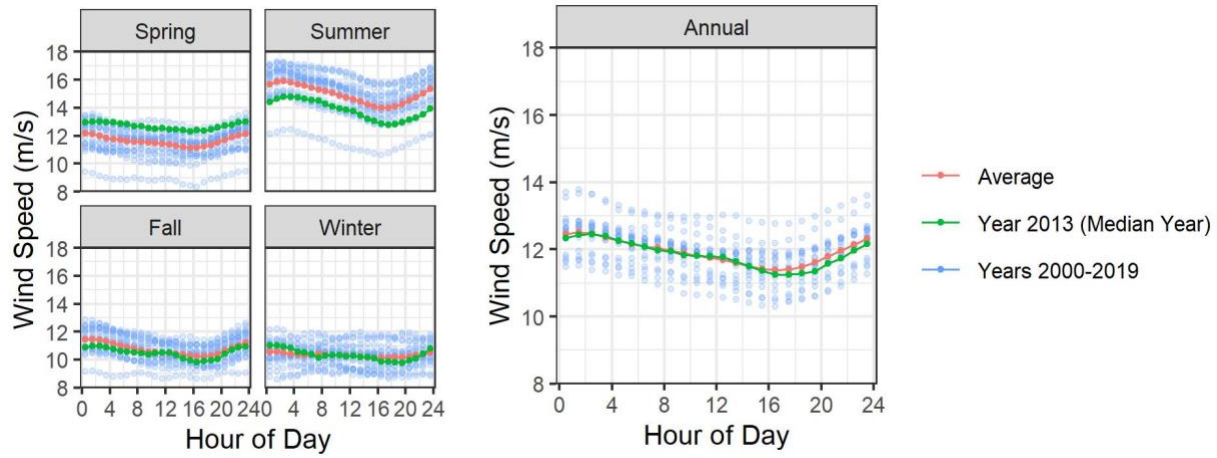

Figure 21. Daily profile of average wind speed at 138 m for the year (right) and by season (left) for the notional Cape Mendocino area. The dots represent data averaged for each of the seven years with the average and median years highlighted in red and green, respectively. Note that the annual average plot does not have the same axis limits as the individual seasonal plots.

The daily profile at the notional Crescent City area in Figure 22 shows a flat daily trend across the seasons. Here, the median year is farther from the mean due to a cluster of low wind speed years.

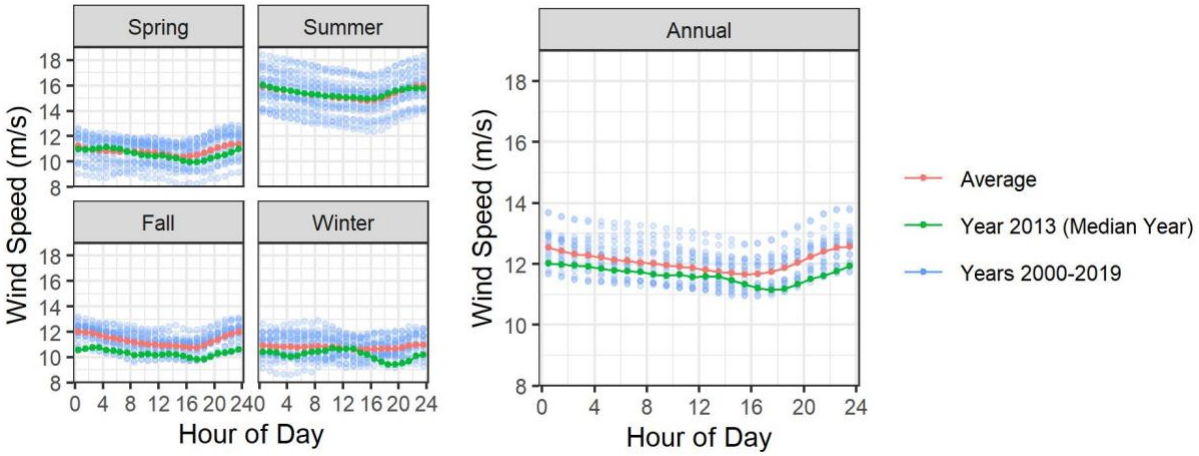

Figure 22. Daily profile of average wind speed at 138 m for the year (right) and by season (left) for the notional Crescent City area. The dots represent data averaged for each of the seven years, with the average and median years highlighted in red and green, respectively. Note that the annual average plot does not have the same axis limits as the individual seasonal plots.

4.3.4 Power Generation

Power generation profiles for the different wind farm scenarios were calculated after applying all loss factors. Table 12 summarizes annual energy production two ways: First, in terms of confidence interval, describing the precision of estimating of the true annual mean, and second, in terms of a tolerance interval, which describes where future values of annual mean energy production are likely to fall. On average, the notional Cape Mendocino area, the most powerful location, provides 16% more generation than the potential study area to the east of the Humboldt Call Area, 10 to 11% more than the centroid of the Humboldt Call Area, and 5% more than the notional Crescent City area.

Table 12. Annual energy production (AEP) summary for Study C wind farm scenarios. The model uses the CA20 dataset and new turbine curve and wake losses and infers power from wind speed at 140 m. n = 20 years.

Site	Size (MW)	AEP 95% Confidence Interval (GWh per yr)	AEP 95% Tolerance Interval (GWh per yr)
Cape Mendocino	48	242 +/- 5.39	210 to 273
Crescent City	48	230 +/- 4.59	203 to 257
Humboldt Call Area	48	219 +/- 5.47	187 to 251
Humboldt Study Area	48	208 +/- 5.57	175 to 241
Cape Mendocino	144	719 +/- 16	625 to 814
Crescent City	144	685 +/- 13.6	604 to 765
Humboldt Call Area	144	652 +/- 16.3	556 to 747
Cape Mendocino	288	1,440 +/- 32	1,250 to 1,620
Crescent City	288	1,370 +/- 27.2	1,210 to 1,530
Humboldt Call Area	288	1,300 +/- 32.5	1,110 to 1,490
Cape Mendocino	480	2,390 +/- 53.3	2,070 to 2,700
Crescent City	480	2,270 +/- 45.3	2,000 to 2,540
Humboldt Call Area	480	2,160 +/- 54	1,840 to 2,480
Cape Mendocino	1836	9,110 +/- 203	7,910 to 10,300
Crescent City	1836	8,650 +/- 172	7,640 to 9,660
Humboldt Call Area	1836	8,230 +/- 206	7,020 to 9,440

Capacity factors are calculated by dividing the total energy production by the theoretical maximum energy production, i.e., the nameplate capacity times 8760 hours per year. This leads to the capacity factors in Table 13. Trends follow the analysis of annual energy production because capacity factor and total production are linearly scaled.

Table 13. Capacity factor (CF) summary for Study C wind farm scenarios. The model uses the CA20 dataset and new turbine curve and wake losses and infers power at 138 m from wind speed at 140 m. n = 20 years.

Region	Size (MW)	CF 95% Confidence Interval	CF 95% Tolerance Interval
Cape Mendocino	48	0.575 +/- 0.013	0.500 to 0.650
Crescent City	48	0.548 +/- 0.011	0.483 to 0.612
Humboldt Call Area	48	0.521 +/- 0.013	0.444 to 0.597
Humboldt Study Area	48	0.494 +/- 0.013	0.417 to 0.572
Cape Mendocino	144	0.570 +/- 0.013	0.495 to 0.645
Crescent City	144	0.543 +/- 0.011	0.479 to 0.606
Humboldt Call Area	144	0.517 +/- 0.013	0.441 to 0.593
Cape Mendocino	288	0.569 +/- 0.013	0.494 to 0.644
Crescent City	288	0.541 +/- 0.011	0.478 to 0.605
Humboldt Call Area	288	0.515 +/- 0.013	0.439 to 0.591
Cape Mendocino	480	0.568 +/- 0.013	0.493 to 0.642
Crescent City	480	0.540 +/- 0.011	0.477 to 0.603
Humboldt Call Area	480	0.514 +/- 0.013	0.438 to 0.589
Cape Mendocino	1836	0.566 +/- 0.013	0.492 to 0.640
Crescent City	1836	0.538 +/- 0.011	0.475 to 0.601
Humboldt Call Area	1836	0.512 +/- 0.013	0.437 to 0.587

Once the shape of the turbine power curve is considered, the differing shapes of wind speed eCDFs, depicted in Figure 14, vanish, and power-duration curves take on similar shapes, as shown in Figure 23. While all four sites apparently generate no power for the same amount of time, the most striking feature of the figure is the steady decrease in time spent at full power moving from the notional Cape Mendocino area to the notional Crescent City area, to the Humboldt Call Area, and finally, the notional Humboldt Study Area.

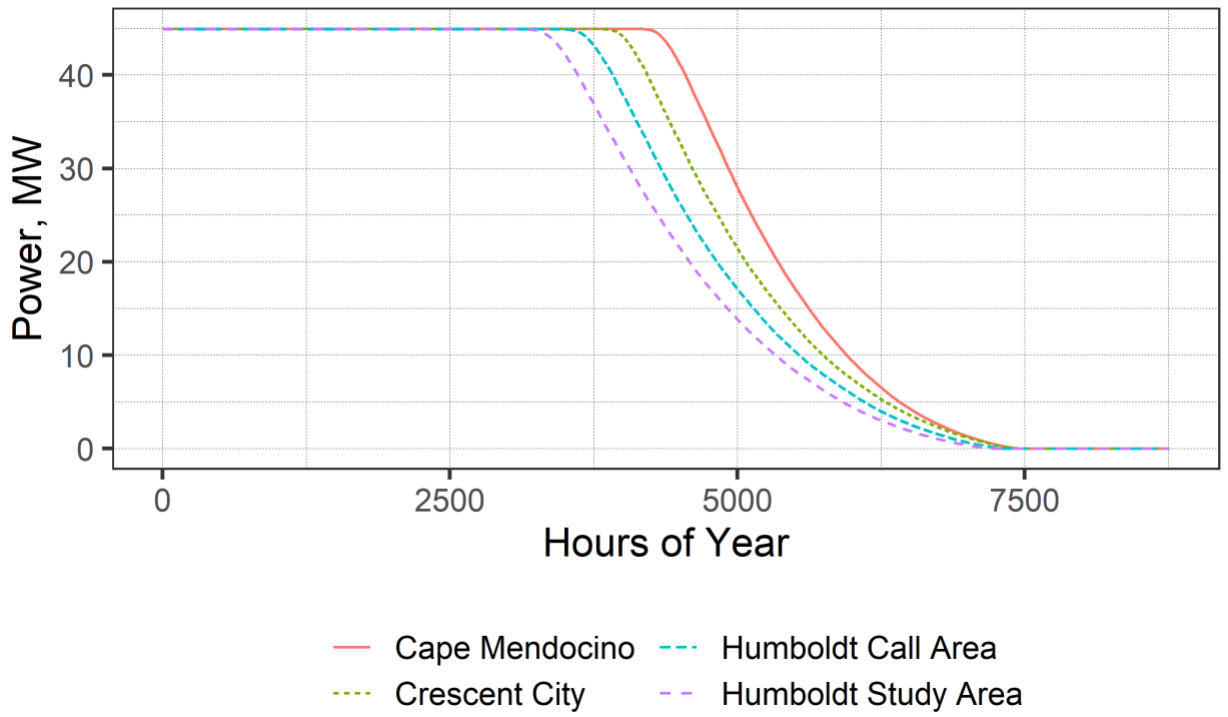

Figure 23. Generation duration curves for all four Study C locations at a scale of 48 MW. Other development sizes have similarly shaped curves, varying only by the scale of power output, and slightly due to differing wake losses.

To illustrate the ways which a 144-MW wind farm located at the Humboldt centroid might perform during normal operation, Figure 24 shows the resulting power production time series for a period of five weeks. The first two weeks are highly intermittent, with spikes of full and nearly-zero power. This is followed by a brief period of very little wind, and then almost a week of nearly continuous full power. Finally, the last two weeks show a period of consistently near-zero generation (with one brief peak of higher power output). Note that this particular period was chosen to depict each of these three different "regimes"; it should not be assumed that a general period chosen at random would exhibit the same, or even similar distributions.

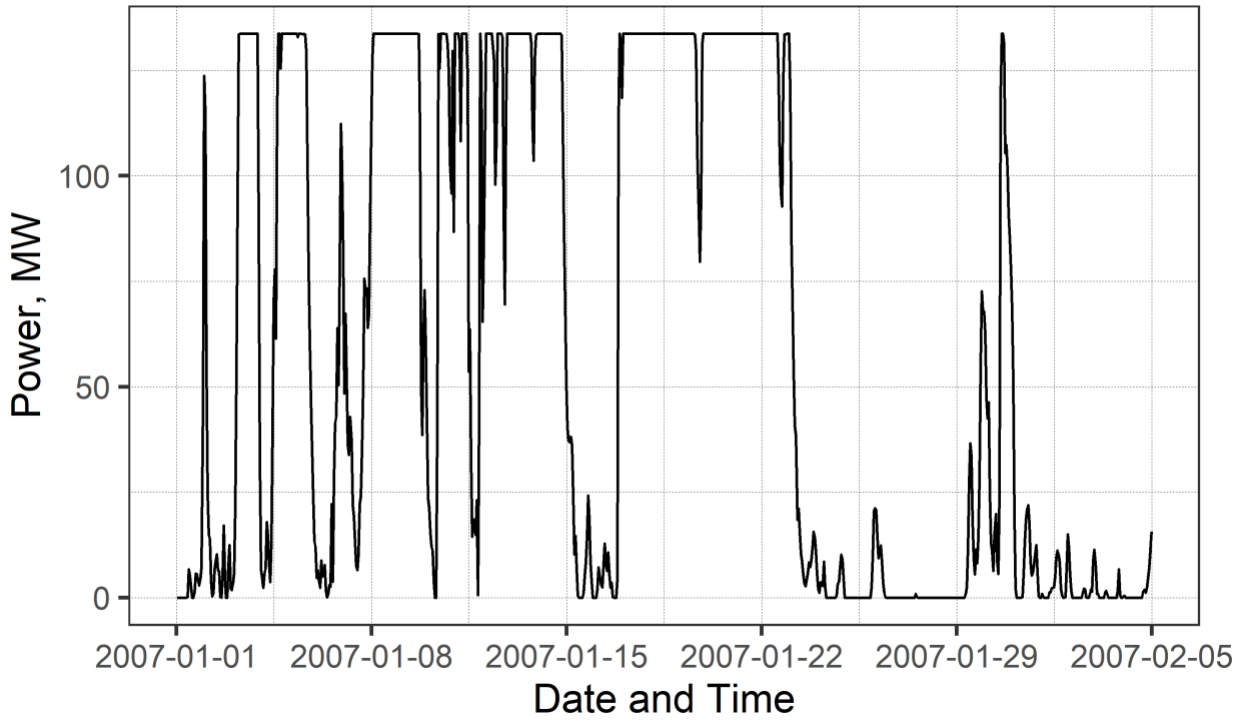

Figure 24. Variability of power production patterns over five weeks in the Humboldt Call Area. These data omit the randomly situated shut-off losses for clarity.

The power generation time series are useful to help understand how wind farms can interact with the transmission grid. Wind generation can vary greatly from day-to-day and week-to-week. The low and high generation days are typical for the spring and summer. However, even during the late fall and winter, power generation can fluctuate quickly between maximum power output and zero power output when the wind speeds exceed the cut-out speed of the turbine. Although the wind speeds only exceed the cut-out velocity 0.5% of the time in the notional Crescent City area, 0.3% of the time in the Humboldt Call Area, and 0.1% of the time in the notional Cape Mendocino location (see Figures 8, 9 & 17), this can have a significant impact on grid operators when the wind speed exceeds 30 meters per second and the entire wind farm must shut down for several hours until it is safe to restart.

The hourly distribution of the power output from wind farms changes by season. Figures 25 to 27 show the frequency of different power output levels by time-of-day for the 144-MW scenarios at the three Study C centroids. Each line represents a different percent likelihood of occurrence, specifically 10%, 25%, 50% (the median), 75%, and 90%. The green dashed line, at the interface between the blue and green range, shows the median power output or 50th percentile. Half of the time power output will be above this level, and half of the time it will be below this level. The power generation that corresponds to the area between the 25% and 75% lines would also occur 50% of the time.

Most notable, the hourly distribution plots show the extreme spread between the maximum and minimum power output. In all seasons, at all locations, both the 75th and the 90th percentiles extend to the maximum output, indicating that for at least 25% of the time the wind array is at maximum capacity. Even further, the 50th percentile reaches the maximum output for the entire

day during the summer in all areas. On the bottom of each chart, the 10th percentile for all seasons, all locations, and all times-of-day always rests at or very near to 0-MW output, and in many hours outside of summer, the 25th percentile is below 25 MW. This is notably different in summer in the notional Cape Mendocino area, where the 25th percentile line extends quite high. One main takeaway from these charts is that power is broadly distributed between the maximum and minimum at all hours of the day, mirroring what was observed from the generation duration curves.

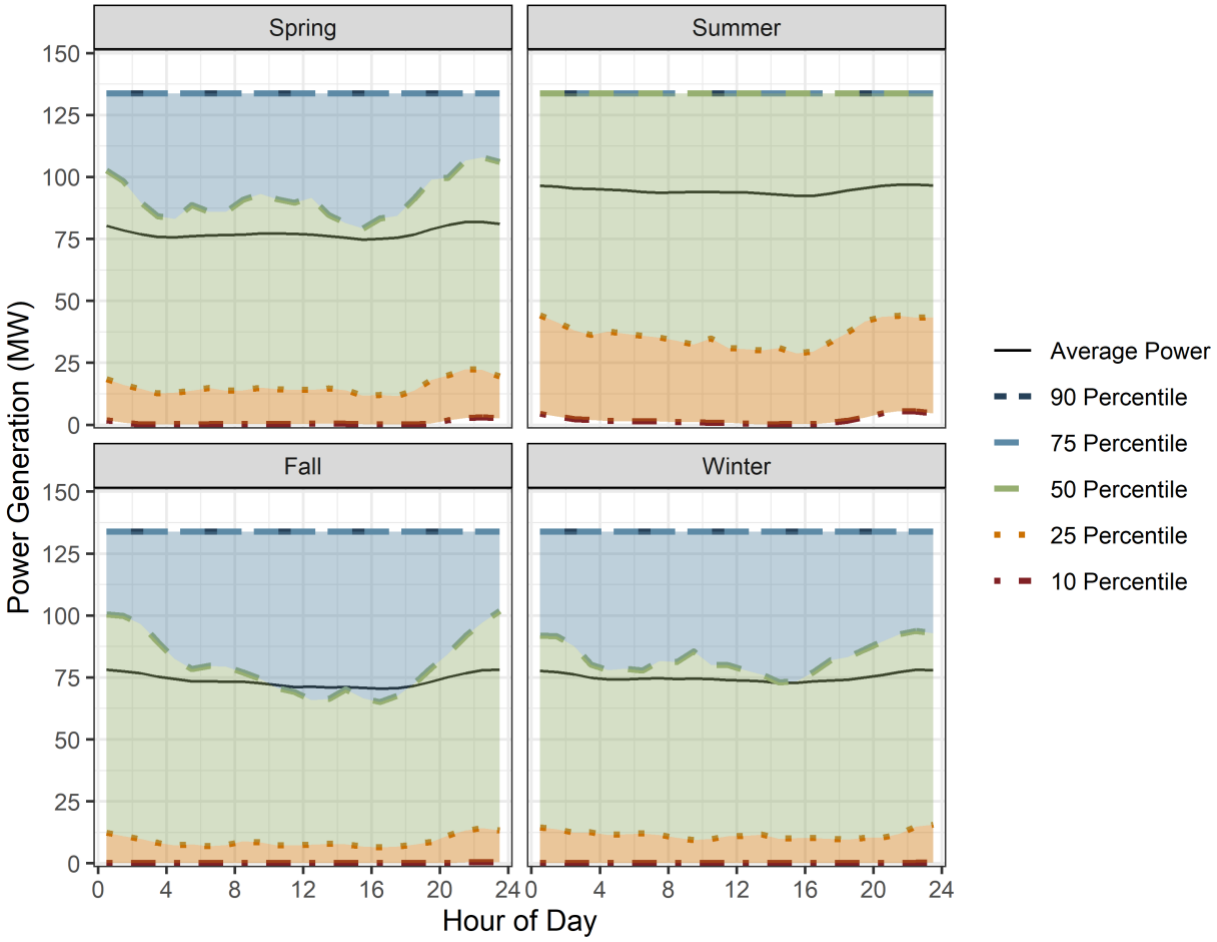

Figure 25. Hourly power generation of the 144-MW farm at the centroid of the Humboldt Call Area by season.

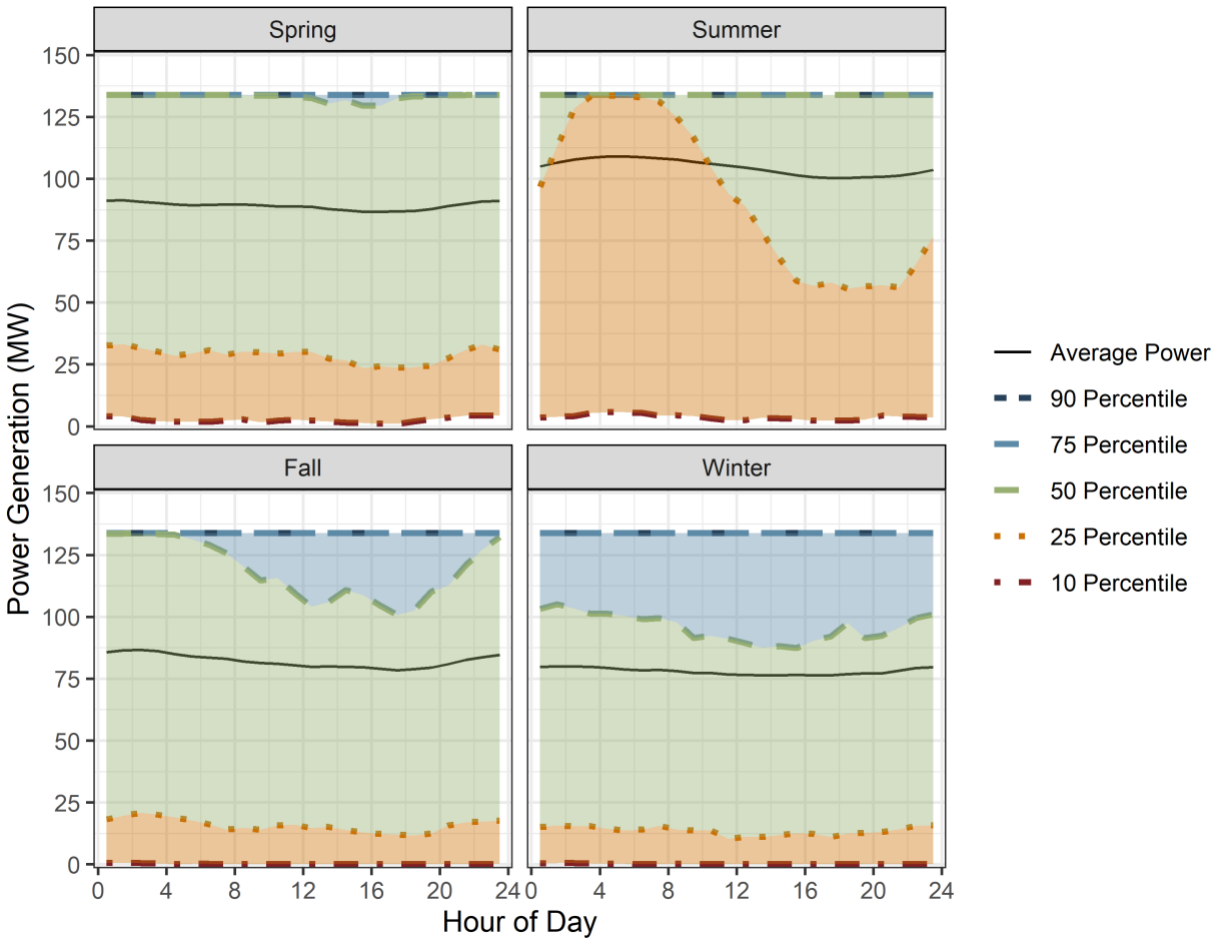

Figure 26. Hourly power generation of the 144-MW farm in the notional Cape Mendocino area by season.

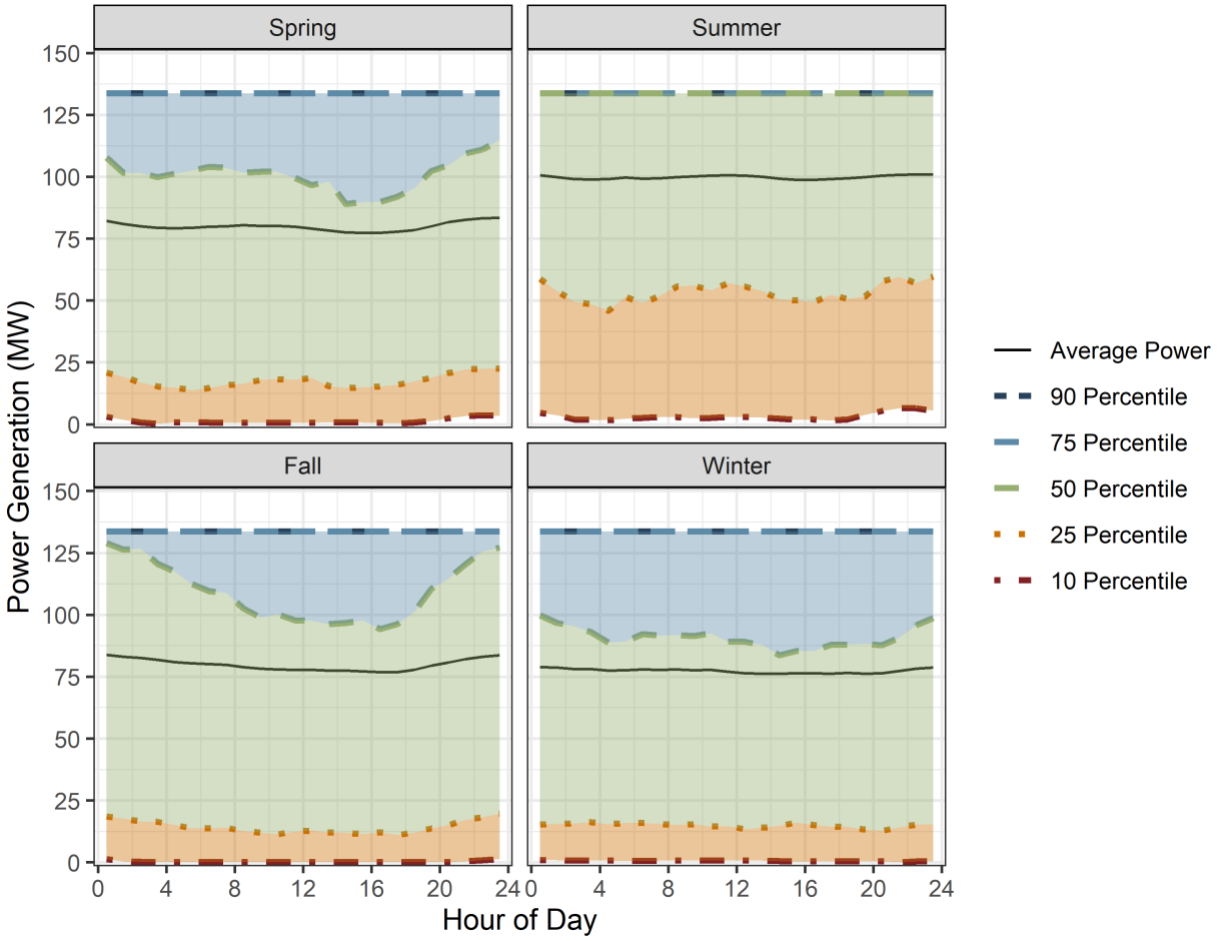

Figure 27. Hourly power generation of the 144-MW farm in the notional Crescent City area by season.

5 DISCUSSION

The updated CA20 wind dataset results in more frequent predictions of higher wind speeds at both the Humboldt Call Area and the hypothetical Cape Mendocino area, as explored in Study A. Significantly, the divergence in empirical cumulative distribution functions begins at about 11 meters per second in the notional Cape Mendocino area, and closer to 9 meters per second in the Humboldt Call Area (see Figure 5). Because at 11 meters per second the turbines are at rated speed, and thus no longer produce more power with increased speed (Figure 1), the new model has little effect on predicted power generation at the notional Cape Mendocino location, while predicting 5 to 6% greater power output in the Humboldt Call Area than the previous model (see Table 8). This reduces the power production advantage in the notional Cape Mendocino area from 17% to 10 to 11% (depending upon development size).

Study B explored the changes in wind speed and power production moving across the Humboldt Call Area from the centroid of a hypothetical east-adjacent farm to that of a hypothetical west-adjacent 480-MW farm. Differences in wind speeds are barely visible (Figure 12), while power production differs by only 2% (Table 10). Across the entire Humboldt Call Area, as shown in Appendix A, power production would vary up to 5%.

The notional Crescent City and Cape Mendocino areas and the Humboldt Call Area all have differently shaped wind speed distributions (Figures 14 & 15), with the notional Cape Mendocino area having the highest occurrence of wind speeds from 15 to 20 meters per second, and the notional Crescent City area having the highest occurrence of speeds above 20 meters per second. Seasonally, the Humboldt Call Area shows the least variation in wind speeds (Figure 16), while the notional Crescent City and Cape Mendocino areas show more significant increases in summer wind speeds. All three sites show about 1 meter per second of diurnal variation regardless of season (Figures 20 to 22). On average, the notional Cape Mendocino area, the most powerful location, provides about 16% more generation than the potential study area to the east of the Humboldt Call Area, 10 to 11% more than the centroid of the Humboldt Call Area, and 5% more than the notional Crescent City area (Table 12). While all four sites apparently generate no power for the same amount of time, there is a steady decrease in time spent at full power moving from the notional Cape Mendocino area to the notional Crescent City area, to the Humboldt Call Area, and finally, the notional Humboldt Study Area (Figure 23).

6 Conclusions and Next Steps

With the newest data and modeling methods, we find that of the three possible development regions, the notional Cape Mendocino area, the most powerful region, would generate 11% more energy than an equally sized development in the Humboldt Call Area, and 5% more than one in the notional Crescent City area. A 48-MW study project outside of the Humboldt Call Area to the east would generate 95% of the power of an equally sized development at the Humboldt Call Area's centroid, while variations within the Call Area are as large as 5% edge-to-edge, or 2% for possible mid-scale, 480-MW developments adjacent to the east and west edges of the Call Area.

In our newest analysis, the power output gap between the notional Cape Mendocino area and the Humboldt Call Area has shrunk significantly, from 17% to 10 to 11%, due to the increased wind speeds predicted by the CA20 model providing more benefit at the Humboldt Call Area based on the turbine power curves we utilized. This highlights the potential value of developing and deploying wind turbines with a power curve that is tailored to these wind regimes (i.e., so that there is greater ability to take advantage of the higher wind speeds). This could prove a valuable topic for future research, having the potential to lead to decreased costs for wind energy offshore of California.

There is potential benefit to a study of more possible locations and more development sizes within the Humboldt Call Area and the other hypothetical call areas. Such studies could be used to inform cost-benefit analyses exploring the tradeoffs of higher wind speed and higher development (and operations and maintenance) costs further from shore.

Furthermore, as mentioned in the introduction, it will be beneficial to validate the CA20 model using lidar data from the recently deployed offshore buoys near the Humboldt Call Area and Morro Bay, which began collecting data in September and October of 2020 (Showalter, 2020).

REFERENCES

AWS Truepower. (2014, June 5). *AWS Truepower Loss and Uncertainty methods*. https://aws-dewi.ul.com/assets/AWS-Truepower-Loss-and-Uncertainty-Memorandum-5-Jun-2014.pdf

Beiter, P., Musial, W., Duffy, P., Cooperman, A., Shields, M. (ORCID:0000000206983816), Heimiller, D., & Optis, M. (ORCID:0000000156176134). (2020). *The Cost of Floating Offshore Wind Energy in California Between 2019 and 2032* (NREL/TP-5000-77384). National Renewable Energy Lab. (NREL), Golden, CO (United States). https://doi.org/10.2172/1710181

Bureau of Ocean Energy Management. (2018a). *Northern California Call Area*. https://www.boem.gov/sites/default/files/renewable-energy-program/State-Activities/CA/Humboldt-Call-Area-Map-NOAA-Chart.pdf

Bureau of Ocean Energy Management. (2018b). *Commercial Leasing for Wind Power Development on the Outer Continental Shelf (OCS) Offshore California-Call for Information and Nominations (Call)*. https://www.federalregister.gov/documents/2018/10/19/2018-22879/commercial-leasing-for-wind-power-development-on-the-outer-continental-shelf-ocs-offshore

Churchfield, M., J. (2013). *A Review of Wind Turbine Wake Models and Future Directions* (NREL/PR-5200-60208). National Renewable Energy Laboratory. https://www.nrel.gov/docs/fy14osti/60208.pdf

Gorton, A. M. (2020a). *Lidar—California—Leosphere Windcube 866 (120), Humboldt* [Data set]. Atmosphere to Electrons (A2e) Data Archive and Portal, Pacific Northwest National Laboratory; PNNL. https://doi.org/10.21947/1671052

Gorton, A. M. (2020b). *Lidar—California—Leosphere Windcube 866 (130), Morro Bay* [Data set]. Atmosphere to Electrons (A2e) Data Archive and Portal, Pacific Northwest National Laboratory; PNNL. https://doi.org/10.21947/1669352

Gorton, A. M. (2021, March 30). *Lidar—California—Leosphere Windcube 866 (120), Humboldt*. https://web.archive.org/web/20210330222103/https://a2e.energy.gov/data/buoy/lidar.z05.00

Masters, G. M. (2013). *Renewable and efficient electric power systems* (Second edition). John Wiley & Sons Inc.

Musial, W., Beiter, P., Nunemaker, J., Heimiller, D., Ahmann, J., & Busch, J. (2019). *Oregon Offshore Wind Site Feasibility and Cost Study* (NREL/TP-5000-74597, 1570430; p. NREL/TP-5000-74597, 1570430). National Renewable Energy Laboratory. https://doi.org/10.2172/1570430

Musial, W., Heimiller, D., Beiter, P., Scott, G., & Draxl, C. (2016). *2016 Offshore Wind Energy Resource Assessment for the United States* (NREL/TP--5000-66599, 1324533; p. NREL/TP--5000-66599, 1324533). https://doi.org/10.2172/1324533

NREL. (n.d.). *Wind Integration National Dataset Toolkit*. Retrieved January 12, 2021, from https://web.archive.org/web/20201118015946/https://www.nrel.gov/grid/wind-toolkit.html

Optis, M., Rybchuk, O., Bodini, N., Rossol, M., & Musial, W. (2020). *2020 Offshore Wind Resource Assessment for the California Pacific Outer Continental Shelf* (NREL/TP-5000-77642, 1677466, MainId:29568; p. NREL/TP-5000-77642, 1677466, MainId:29568). https://doi.org/10.2172/1677466

Severy, M., Ortega, C., Chamberlin, C., & Jacobson, A. (2020). Wind Speed Resource and Power Generation Profile Report. In M. Severy, A. Younes, J. Zoellick, M. Cheli, C. Ortega, T. Garcia, G. Chapman, N. Salas, Z. Alva, & A. Jacobson (Eds.), *California North Coast Offshore Wind Studies*. Schatz Energy Research Center. schatzcenter.org/pubs/2020-OSW-R2.pdf

Showalter, M. A. (2020, October 9). *Offshore Wind Research Buoys Float into California's Waters | PNNL*. https://www.pnnl.gov/news-media/offshore-wind-research-buoys-float-californias-waters

Appendix A POWER PRODUCTION TRANSECT

This appendix explores the predicted power production across the entire width of the Humboldt Call Area, as shown in Figure A-1. In this chart, larger absolute values of the x-axis correspond with locations that are further westward, so the left and right sides follow the convention of a normal map. The far west side generates 5% more power than the far east side, in a shape that is not entirely linear but close to it over this distance. The longitudes of the east and west Humboldt Call Area centroids are shown for reference in red, along with their interpolated power production.

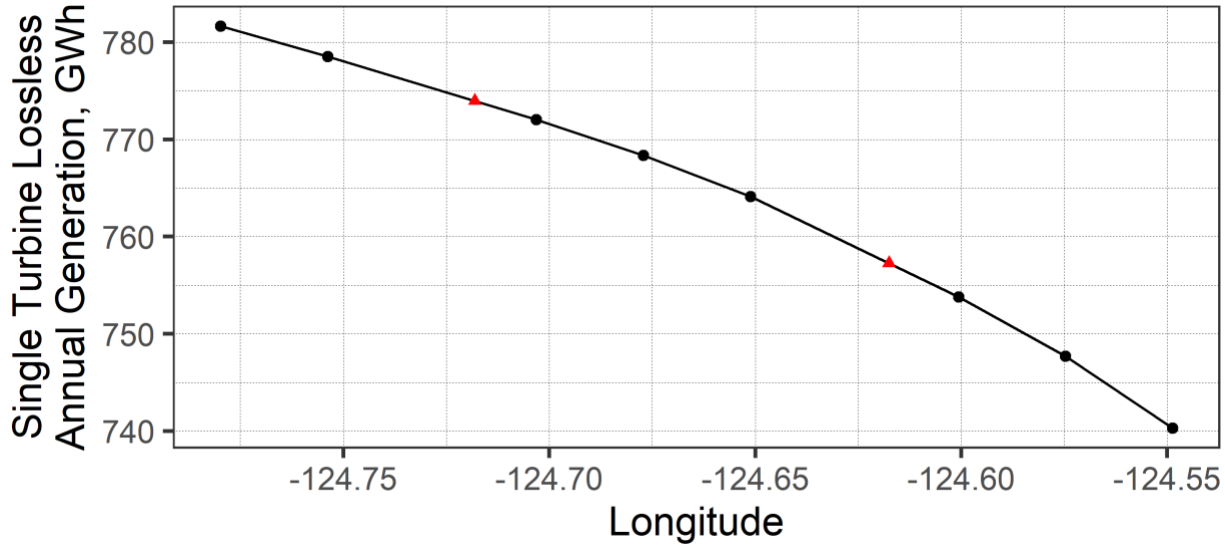

Figure A-1. Power generation for a single turbine in the Humboldt Call Area as a function of longitude, for the year 2014 before considering power losses. Red triangles indicate the longitudes and interpolated power production of the east and west centroids used in Study B. Note that the y axis does not include zero, thus exaggerating differences.

Appendix B LOSS FACTORS

This appendix provides a table of loss factors, reprinted in part from Severy et al. (2020), in Table B-1.

Table B-1. Power loss factors.

Loss Origin	Loss Factor	Depends On	Effect on Model
Internal Wake Effect of the Project [a]	Varies	Wind farm scale and density, see Table 7.	Even reduction
Wake Effect of Existing or Planned Projects [a]	0.0%		Even reduction
Contractual Turbine Availability [a]	3.0%	O&M plan; Proven reliability/ newness of turbine	Turn to 0 MW
Non-contractual Turbine Availability [a]	1.3%		Turn to 0 MW
Availability Correlation with High Wind Events [a]	1.3%	Frequency of high wind events	Turn to 0 MW
Availability of Collection & Substation [a]	0.2%	Timing of substation downtime	Turn to 0 MW
Availability of Utility Grid [a]	0.3%	Timing of grid blackouts	Turn to 0 MW
Plant Re-start after Grid outages [a]	0.2%	Timing of grid blackouts	Turn to 0 MW
First-Year Plant Availability [a]	0.0%		
Electrical Efficiency [a]	2.0%	Distance between turbines and substation	Even reduction
Power Consumption of Weather Package [a]	0.1%		Even reduction
Sub-optimal operation [a]	1.0%		Even reduction
Power Curve Adjustment [a]	2.4%		Even reduction
High Wind Control Hysteresis	1.0%	Wind regime at site; turbine model	Turn to 0 MW
Inclined Flow [a]	0.0%		Even reduction
Icing [a]	0.0%*	Temperature	Turn to 0 MW
Blade Degradation [a]	1.0%		Even reduction
Low/High Temperature Shutdown [b]	0.0%*	Temperature, turbine limits	Turn to 0 MW
Site Access [a]	0.1%	O&M plan, availability of parts, staff, vessels	Turn to 0 MW
Lightning [b]	0.1%		Turn to 0 MW
Directional Curtailment [a]	0.0%	Layout and spacing	Turn to 0 MW
Environmental Curtailment [a]	0.0%	Local environmental regulation	Turn to 0 MW
PPA Curtailment [a]	0.0%	Wind farm scale and density	Turn to 0 MW
Pre-Wake Total	**13.2%**		

Appendix C QUANTILE-QUANTILE PLOTS OF CAPACITY FACTORS

This appendix provides a quantile-quantile plot of capacity factor intended to show (Figure C-1) that the distributions of the capacity factors are at least qualitatively normally distributed, a requirement of calculations of confidence intervals and tolerance intervals given in the main body of the report. As noted, while these data represent the annual capacity factor for a 144 MW development specifically, all other development sizes and output variables (annual energy production) for these locations are linearly scaled from these results, and thus would have the same distributions.

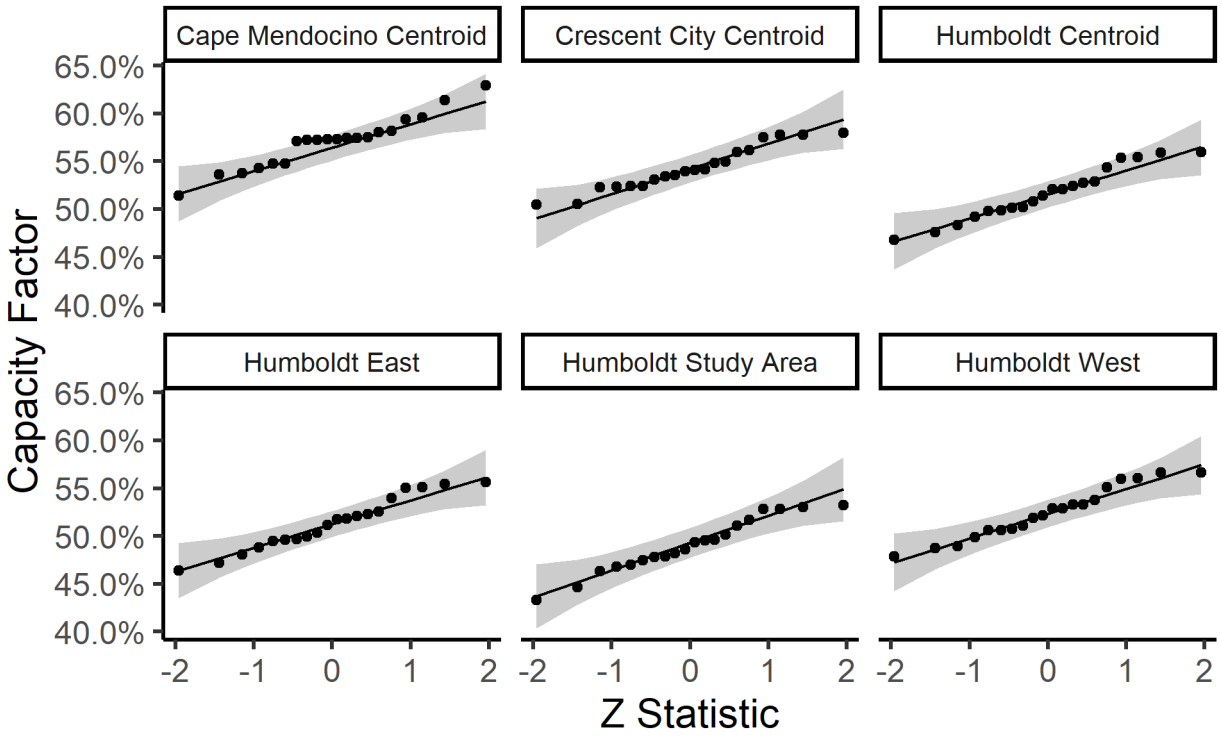

Figure C-1. Quantile-Quantile plots of annual capacity factor for a 144-MW development at each prospective site.